LRP 675/00 August 2000

Effect of Helical Coils on the Magnetic Field and the Stability of a Compact Toroidal Plasma

W.A. Cooper, T.N. Todd, S. Allfrey,
T.C. Hender, D.C. Robinson

Accepted for publication in
Plasma Physics and Controlled Fusion

ISSN 0458-5895

EFFECT OF HELICAL COILS ON THE MAGNETIC FIELD AND THE STABILITY OF A COMPACT TOROIDAL PLASMA

W. A. COOPER
Centre de Recherches en Physique des Plasmas, Association Euratom-Confédération Suisse, Ecole Polytechnique Fédérale de Lausanne, CRPP-PPB, CH-1015 Lausanne, Switzerland

T. N. TODD, S. ALLFREY, T. C. HENDER, D. C. ROBINSON
Euratom/UKAEA Fusion Association, Culham Science Centre, Abingdon Oxon OX14 3DB, UK

Abstract

The helical distortion of a compact tokamak plasma with currents in modular Furth-Hartman type coils is investigated with respect to the impact on the magnetic field structure and to the ideal magnetohydrodynamic stability. A sequence of configurations in which the current in the helical coils is increased up to the level of that of the main toroidal coils is generated. The magnetic field structure acquires a ripple along the field lines when the currents in both sets of coils becomes comparable. The magnitude of this ripple depends on the modulation of the Furth-Hartman coils on their winding surface. The local ideal ballooning stability properties deteriorate with increasing helical deformation of the plasma shape because the normal magnetic field line curvature becomes larger in regions where the helical contribution enhances the toroidicity component while the local magnetic shear vanishes. The global external kink stability properties, on the contrary, improve because the normal curvature on average does not change while the local magnetic shear acquires a noticeable helical modulation.

1 INTRODUCTION

Spherical Tokamak (ST) devices have demonstrated many favourable physics properties such as high β operation with naturally large elongation, resiliency against disruption, etc [1]. In reactor-scale devices, however, the tight aspect ratio of the ST leads to a central aperture which is too small for a shielded superconductiong toroidal field coil and so a minimally neutron shielded normal conductor (eg a copper alloy) must be employed with the penalty of high resistive power dissipation. The utilisation of appropriately designed helical windings could relieve some of the constraints that are imposed by the tight aspect ratio of the structure.

In this article, we shall examine a compact tokamak system with an additional set of stellarator windings on the outboard side of the tokamak cross section that were first proposed by Furth and Hartman [2]. In Ref. [2], it was shown that in the large aspect ratio limit the currents in these windings enhance the magnetic well which could have favourable implications for magnetohydrodynamic (MHD) stability. A follow-up paper demonstrated that these types of coils could yield a stellarator-spheromak hybrid with potentially interesting physical properties [3]. A

further extension of this concept is the Sphellamak [4] where it is shown that the outboard helical coils produce a toroidal translation of the magnetic field lines and seed paramagnetism. Three dimensional (3D) equilibrium studies demonstrated that the toroidal plasma current generated a strong paramagnetic enhancement of the magnetic field, that peaked toroidal plasma currents yielded nearly isodynamic [5] conditions in the plasma core and that hollow toroidal plasma currents produced quasiaxisymmetric systems [6]. A somewhat different concept has been considered in which the currents in the outboard helical coil structures flow in the same sense [7]. All these configurations explored are characterised by the absence of a linked central conductor. Here, we are interested in the investigation of a ST system in conjunction with a set of Furth-Hartman coils that generate a fraction of the confining magnetic fields such that the symmetry properties of these fields are not profoundly altered. Alternatively, we can describe the system as a Sphellamak with toroidal field (TF) coils. The aspect ratio of the configurations we investigate in this work, however, are not as tight as typical ST devices. They could be more appropriately referred to as a hybrid between a Compact Tokamak (CT) and a Sphellamak. A similar system, the stellarator-spheromak, was proposed and its 3D equilibrium properties investigated [8]. The configurations identified, however, can be more closely identified with classical stellarators because the magnetic field distribution displays a more noticeable 3D structure than the systems examined in this paper. The study of the stabilisation of a quasiaxisymmetric stellarator as a result of 3D shaping effects has been investigated in detail at PPPL [9-11]. This system achieves better symmetry than the device we consider, but at a larger aspect ratio. Improvement of vertical stability conditions is realised through the external poloidal magnetic flux [12].

The coil description of the CT/Sphellamak hybrid device is presented in Sec. 2. The determination of 3D equilibria that models the basic CT/Sphellamak hybrid that is marginally stable to local ideal MHD modes is described in Sec. 3. The properties of the magnetic field in the sequence of configurations investigated is discussed in Sec. 4. The global external ideal MHD kink stability behaviour of the sequence is considered in Sec. 5 and the summary and discussion appears in Sec. 6.

2 COIL DESCRIPTION

The configuration consists of 10 toroidal field coils wound on a spherical structure of $1.1m$ radius with a $0.5m$ diameter core removed. Inside the toroidal coils, 10 modular helical Furth-Hartman type coils are wound on a sphere of $1m$ and modulated toroidally so that the maximum inclination from the vertical is at the midplane. Typically, the toroidal angle position of a filament segment $v_\ell(t)$ of this coil set as a function of the angular variable t that governs its motion from the polar region (where $t \longrightarrow 0$) to the equator (where $t \longrightarrow \pi/2$ is given by $v_\ell(t) = -\alpha(t - t_{max}) + \nu sin[\pi(t - t_{min})/(t_{max} - t_{min})]$, where α is the average pitch of the filament, ν controls the modulation of the filament on the winding surface,

where $\delta_p << 1$ is a small contribution that makes the pressure gradient finite at the magnetic axis and the plasma edge to facilitate the convergence towards an equilibrium. In this work, we define the plasma β value as

$$\beta = \frac{2\mu_0 \int d^3x p}{\int d^3x B^2} . \tag{3}$$

We subsequently apply the local stability modules of the TERPSICHORE code [15,16] to determine the ballooning and Mercier stability eigenvalues and iteratively flatten the pressure profile in the unstable regions until marginal conditions are achieved. This procedure is carried out for a sequence of configurations in which the current in the helical coils I_{hc} is $20kA$, $60kA$, $120kA$ and $180kA$. The toroidal plasma current is adjusted to keep the inverse rotational transform (safety factor) fixed at $q \simeq 2.2$ at the edge. The corresponding toroidal plasma current values are $2\pi J(1) = -265kA$, $-262.5kA$, $-259kA$ and $-250kA$, respectively. The value of the pressure on axis $p(0)$ is changed so that $\beta \simeq 14.4\%$ remains fixed. For the nearly axisymmetric case, this value of β corresponds approximately to a normalised $\beta_N = 7\%Tm/MA$. The mod-B distribution on 3 cross sections at the beginning, at one quarter and at midperiod calculated with the VMEC code for the four configurations examined is presented in Fig. 3. The results show that the plasma shape acquires a significant three dimensional shape when $I_{hc} \geq 120kA$. However, the mod-B structure in the VMEC coordinates appears to be only weakly modified. The initial and ballooning stable pressure profiles for the near axisymmetric $I_{hc} = 20kA$ and for the 3D $I_{hc} = 180kA$ systems are displayed in Fig. 4. The corresponding inverse rotational transform profiles are shown in Fig. 5. The nearly axisymmetric configuration requires only minor modifications to the plasma pressure and the resulting alterations to the inverse rotational transform profile are small. The more fully 3D case, however, requires a marked flattening of the pressure profile around the vanishing global magnetic shear region near the edge of the plasma to assure local ideal MHD stability and the corresponding alterations to the inverse rotational transform profile become quite significant at fixed β.

4 THE MAGNETIC FIELD STRUCTURE

The variation of the current in the helical coils destroys the toroidal axisymmetry of the system when it approaches the value of the current in the TF coils as Fig. 3 demonstrates. The magnetic field structure, however, appears to retain approximately the toroidal symmetry conditions. To show this, we refer to Fig. 6 which plots the five largest Fourier amplitudes of B^2 calculated in Boozer magnetic coordinates [17] as a function of the radial variable s for the nearly axisymmetric ($I_{hc} = 20kA$) and 3D CT/Sphellamak hybrid ($I_{hc} = 180kA$) configurations. The dominant Fourier amplitudes of B^2 in the near axisymmetric case all have toroidal mode number $n = 0$, as expected. When the current in the helical coil structure becomes comparable to the TF coil current, the largest symmetry breaking term

in the spectrum corresponds to a mirror component $m/n = 0/10$ (m is the poloidal mode number). This component, however, is nearly vanishing in the outer half of the plasma volume ($0.5 < s < 1$) and small compared with the leading $n = 0$ terms in this region. The property that the geometric structure of a configuration is fully 3D while the magnetic field structure is dominated by $n = 0$ components of the spectrum is referred to as quasiaxisymmetry [18,19]. The neoclassical transport properties in such systems are predicted to be very similar to those of the comparable fully axisymmetric state. This is a consequence of the condition that the guiding centre drifts depend only on the magnitude of B and flux surface quantities in the Boozer magnetic coordinate frame [20]. The mod-B^2 distributions on 3 different cross sections that span one half of a field period that appear in Fig. 7 for a nearly axisymmetric case (generated with a helical coil $I_{hc} = 20kA$) and a hybrid case ($I_{hc} = 180kA$) tend to confirm this transition from axisymmetry to quasiaxisymmetry. However, a graph of the magnetic field strength along a field line on a flux surface with $s \simeq 0.9$ (near the edge of the plasma) in Fig. 8 (top figure) demonstrates that the field structure experiences a significant ripple effect that is not readily apparent from the plots of just the five leading components of the B^2 spectrum. Smaller components not shown make a nonnegligible contribution that annihilate the quasiaxisymmetry conditions in the outer part of the plasma imposed by the five dominant components of B^2. Increasing the coil modulation parameter ν reduces the magnitude of the ripple significantly but does not eliminate it completely. As the two main wells along a field line are healed, a secondary set of wells starts to develop. The best result is obtained when $\nu = -0.6$ for which the magnitude of B along the field line is displayed in the middle plot of Fig. 8. For $\nu = -0.9$, the ripple becomes comparable to the $\nu = -0.3$ case. Adding a set of vertical field coils inside the helical coils at about $\pm 0.35m$ off the midplane with $20kA$ of current can almost completely heal the ripple as shown in the bottom graph of Fig. 8. But this is accomplished at the expense of a strong reduction in the plasma volume and, to a lesser extent, a decrease of the 3D shaping of the plasma.

5 GLOBAL EXTERNAL IDEAL KINK STABILITY

The global modules of the TERPSICHORE code [15,16] are employed to evaluate the external ideal MHD kink stability properties of the sequence of configurations we have investigated. The ideal external kink behaviour is very different from that of the local ballooning modes. In all cases considered, a conducting wall is required to stabilise the global current driven modes. Nevertheless, the helical structure that the current in the Furth-Hartman coils imposes on the plasma shape allows the nearly conformal conducting wall to be placed farther away from the plasma-

vacuum interface. This is illustrated in Fig. 9 where the shape of the plasma and the conducting wall is displayed for the nearly axisymmetric case ($I_{hc} = 20kA$) and the hybrid case ($I_{hc} = 180kA$) with helical coil modulation $\nu = -0.3$ at the 3 cross sections previously identified. The critical position of the conducting wall is quantified in Fig. 10 which shows the unstable eigenvalue of a dominant $m/n = 3/1$ external kink plotted as a function of Δ_W, the ratio of the diameter of the conducting wall to that of the plasma at the midplane of the up-down symmetric cross section at the beginning of a field period. The instability structure is computed with 93 mode pairs. Successively removing 11 components of the toroidal sideband with mode number $n = \pm 21$ and another 11 with mode number $n = \pm 19$ does not significantly modify the eigenvalue of -2.5×10^{-3} for the $I_hc = 180kA$, $\Delta_W = 2$ result shown in Fig. 10. Once the $n = \pm 11$ sideband is ignored, the eigenvalue reduces to about -2×10^{-3}. Though many relevant equilibrium quantities in addition to B^2 in the sequence examined appear to retain dominant axisymmetric features, the interaction of the pressure gradient with the normal curvature $2p'(s)\sqrt{g}\boldsymbol{\kappa} \cdot \boldsymbol{\nabla} s$, however, acquires a distinctive helical structure that can destabilise ballooning modes locally both poloidally and toroidally. This is evident in Fig. 11 where the $2p'(s)\sqrt{g}\boldsymbol{\kappa} \cdot \boldsymbol{\nabla} s$ distribution on a toroidal surface with $s \sim 0.75$ which is virtually axisymmetric for $I_{hc} = 20kA$ becomes nonsymmetric for $I_{hc} = 180kA$. Another important equilibrium quantity that is relevant for stability is the local magnetic shear [21] defined by

$$\sqrt{g}S = \psi'(s)\Phi''(s) - \Phi'(s)\psi''(s) - \sqrt{g}\boldsymbol{B} \cdot \boldsymbol{\nabla} h_s \,, \tag{4}$$

where $2\pi\psi$ and $2\pi\Phi$ are the poloidal and toroidal magnetic fluxes, respectively, prime ($'$) denotes the derivative of a flux surface quantity with respect to s, $\sqrt{g}$ is the Jacobian of the transformation to Boozer magnetic coordinates, h_s is the radial component of $\mathbf{h}$ in the covariant representation and $\boldsymbol{h} \equiv \boldsymbol{B} \times \boldsymbol{\nabla} s / |\boldsymbol{\nabla} s|^2$. This expression also acquires a distinct helical modulation roughly aligned with the inclination of the coils which is displayed in the comparison between the $I_{hc} = 20kA$ and $I_{hc} = 180kA$ cases in Fig. 12. For the nearly axisymmetric system, $\sqrt{g}S$ is negative everywhere on the outside edge of the toroidal surface with a minimum value of -0.0005. In the more fully 3D case, this quantity can reach much larger absolute magnitudes, varying between -0.0011 and 0.0004. More importantly, there are regions where it vanishes. The perturbed pressure distribution shows a dominant $m/n = 3/1$ global external kink in Fig. 13 for the two limiting configurations we have explored. The global mode structures, which are closely aligned with the pitch of the magnetic field lines, must work harder to form through the undulations of the local magnetic shear in the 3D hybrid case. Local mode structures that concentrate in the regions where the local magnetic shear vanishes on the outside edge of the torus, on the other hand, can be more easily destabilised.

6 SUMMARY AND CONCLUSIONS

The effect of currents in modular helical Furth-Hartman coils on the magnetic field structure and the ideal MHD stability properties of a compact tokamak configuration have been investigated. When the current in the helical coils exceeds that in the toroidal field coils, the plasma shape acquires a distinctly 3D character. The leading components of the magnetic field spectrum appear to indicate a transition to quasiaxisymmetry, but higher order terms contribute to the formation of a significant ripple feature of the magnetic field strength along a field line. The magnitude of the ripple varies with the modulation of the helical coils on the winding surface. The minimal ripple occurs for the modulation parameter $\nu \simeq -0.6$. Whether the resulting ripple is satisfactory for the confinement of α-particles in a reactor-sized version of the device described here remains to be explored and will be considered in future work. Adequate α-particle confinement is critical for the determination of the relevance of any magnetic plasma confinement system that is proposed for fusion energy production. The local ideal MHD stability properties are deteriorated by the helical deformation of the plasma because it causes the normal magnetic field line curvature to increase in local regions and $\sqrt{g}S$ to vanish. This becomes manifest by the flattening of the pressure profile required to satisfy ballooning and Mercier stability conditions near the edge of the plasma. The global external kink stability properties are improved because on average the normal curvature is unchanged but the local magnetic shear becomes noticeably modulated. This allows the required conducting wall to guarantee stability to be displaced farther away from the plasma. Future work that has motivated this study will explore the conditions that the helical distortion of the plasma shape can provide a significant fraction of the magnetic fields and the rotational transform to relieve the current in the central rod and therefore the corresponding recirculating power without drastically affecting the confinement properties.

Acknowledgments

This research was partially sponsored by the Fonds National Suisse de la Recherche Scientifique, by the United Kingdom Department of Trade and Industry and by Euratom. We thank Dr. S.P. Hirshman for use of the VMEC equilibrium code. The numerical calculations presented in this paper were performed on the NEC-SX4 computer at the Centro Svizzero di Calcolo Scientifico, Manno, Switzerland.

References

[1] SYKES, A., 1999 Nucl. Fusion **39** 1271.

[2] FURTH, H.P., HARTMAN, C.W., 1968 Phys. Fluids **11** 408.

[3] HARTMAN, C.W., 1980 *Stellarmak a Hybrid Stellarator-Spheromak*, in Proc. US-Japan Joint Symposium on Compact Toruses and Energetic Particle Injection, Princeton 1979, UCRL-83792.

[4] TODD, T.N., 1997 *The Sphellamak: a Coreless Spherical Tokamak*, in Proc. 4th International ST Workshop, St. Petersburg, Russia.

[5] PALUMBO, D., 1968 Il Nuovo Cimento X **53B** 507.

[6] COOPER, W.A., ANTONIETTI, J.M., TODD, T.N., 1998 in Proc. 17th IAEA Fusion Energy Conf., Yokohama, Japan, IAEA-CN-69/EX4/1(R).

[7] YAMAZAKI, K., 1982 *Sphelimak: a Helical Spheromak Stabilizing Tilt-Modes*, in Proc. 4th US-Japan Workshop on Compact Toroids, Osaka & Nagoya 230.

[8] MOROZ, P., 1997 Phys. Letters **A236** 79.

[9] REIMAN, A., FU, G., HIRSHMAN, S., KU, L., MONTICELLO, D., MYNICK, H., REDI, M., SPONG, D., ZARNSTORFF, M., BLACKWELL, B., BOOZER, A., BROOKS, A., COOPER, W.A., DREVLAK, M., GOLDSTON, M., HARRIS, J., ISAEV, M., KESSEL, C., LIN, Z., LYON, J.F., MERKEL, P., MIKHAILOV, M., MINER, W., NAKAJIMA, N., NEILSON, G., NÜHRENBERG, C., OKAMOTO, M., POMPHREY, N., REIERSEN, W., SANCHEZ, R., SCHMIDT, J., SUBBOTIN, A., VALANJU, P., WATANABE, K.Y., WHITE, R., 1999 Plasma Phys. Control. Fusion **41** B273.

[10] NEILSON, G.H., REIMAN, A.H., ZARNSTORFF, M.C., BROOKS, A., FU, G.Y., GOLDSTON, R.J., KU, L.P., LIN, Z., MAJESKI, R, MONTICELLO, D.A., MYNICK, H., POMPHREY, N., REDI, M.H., REIERSEN W.T., SCHMIDT J.A., HIRSHMAN, S.P., LYON, J.F., BERRY, L.A., NELSON, B.E., SANCHEZ, R., SPONG, D.A., BOOZER, A.H., MINER, W.H., VALANJU, P.M., COOPER, W.A., DREVLAK, M., MERKEL, P., NÜHRENBERG, C., 2000 Phys. Plasmas **7** 1911.

[11] REDI, M.H., DIALLO, A., COOPER, W.A., FU, G.Y., NÜHRENBERG, C., POMPHREY, N., REIMAN, A.H., ZARNSTORFF, M.C., NCSX TEAM, 2000 Phys. Plasmas **7** 2508.

[12] FU, G.Y., KU, L.P., COOPER, W.A., HIRSHMAN, S.P., MONTICELLO, D.A., REDI, M.H., REIMAN, A., SANCHEZ, R., SPONG, D.A., 2000 Phys. Plasmas **7** 1809.

[13] HIRSHMAN, S.P., VAN RIJ, W.I., MERKEL, P., 1986 Comput. Phys. Commun. **43** 143.

[14] HIRSHMAN, S.P., BETANCOURT, O., 1991 J. Comput. Phys. **96** 99.

[15] ANDERSON, D.V., COOPER, W.A., GRUBER, R., MERAZZI, S., SCHWENN, U., 1990 Int. J. Supercomp. Appl. **4** 34.

[16] COOPER, W.A., 1992 Plasma Phys. Contr. Fusion **34** 1011.

[17] BOOZER, A.H., 1980 Phys. Fluids **23** 904.

[18] NÜHRENBERG, J., LOTZ, W., GORI, S., 1994 *Quasi-axisymmetric Tokamaks*, in Proc. Joint Varenna-Lausanne Int. Workshop on Theory of Fusion Plasmas, Editrice Compositori, Bologna 3.

[19] GARABEDIAN, P.R., 1996 Phys. Plasmas **3** 2483.

[20] BOOZER, A.H., KUO-PETRAVIC, G., 1981 Phys. Fluids **24** 851.

[21] GREENE, J.M., JOHNSON, J.L., 1968 Plasma Phys. **10** 729.

Figures

FIG. 1. The coils system of a Compact Tokamak/Sphellamak hybrid device. The TF coils are shown in blue, the outboard helical coils in green, the compensating VF coils in red and the VF coils in orange.

FIG. 2. The toroidal plasma current profile that is prescribed.

FIG. 3. The mod-B distribution on the toroidal angle $v = 0$ (left), $v = \pi/20$ (middle) and $v = \pi/10$ (right) constant planes of the configurations generated with $I_{hc} = 20kA$, $60kA$, $120kA$ and $180kA$ from top to bottom, respectively. The corresponding toroidal plasma currents are $2\pi J(1) = -265kA$, $-262.5kA$, $-259kA$ and $-250kA$, respectively. These distributions are calculated in the coordinates of the VMEC code and the cross sections shown are at the beginning, at $1/4$ and at $1/2$ of a field period. The volume average β is 14.4%.

FIG. 4. The initial ($\diamondsuit$) and the ballooning stable ($\sqcap$) pressure profiles for the configurations generated with $I_{hc} = 20kA$ (left) and $I_{hc} = 180kA$ (right) at $\beta = 14.4\%$.

FIG. 5. The inverse rotational transport profiles corresponding to the initial ($\diamondsuit$) and the ballooning stable ($\sqcap$) pressure profiles for the configurations generated with $I_{hc} = 20kA$ (left) and $I_{hc} = 180kA$ (right) at $\beta = 14.4\%$.

FIG. 6. The 5 principal Fourier amplitude profiles of B^2 as a function of s computed in Boozer magnetic coordinates for the configurations generated with $I_{hc} = 20kA$ (left) and $I_{hc} = 180kA$ (right) at $\beta = 14.4\%$.

FIG. 7. The mod-B^2 distribution on 3 cross sections at the beginning (left), at $1/4$ (middle) and at $1/2$ (right) of a field period for the configurations generated with $I_{hc} = 20kA$ (top) and $I_{hc} = 180kA$ (bottom) at $\beta = 14.4\%$ computed in Boozer magnetic coordinates.

FIG. 8. The magnitude of the magnetic field strength along a magnetic field line for a configuration with helical coil current $I_{hc} = 180kA$ in which the helical coils have a toroidal modulation parameter $\nu = -0.3$ (top), $\nu = -0.6$ (middle) and $\nu = -0.6$ and an additional vertical field coil set located at $R = 0.8m$ and $Z = \pm 0.35m$ with current $I_s = 20kA$ (bottom).

FIG. 9. The plasma shape (inner contours) and the prescribed conducting wall shape (outer contours) on cross sections at the beginning (left), at $1/4$ (middle) and at $1/2$ of a field period for the configurations generated with $I_{hc} = 20kA$ (top) and $I_{hc} = 180kA$ (bottom) at $\beta = 14.4\%$. The placement of the conducting wall provides marginally stable conditions with respect to dominant $m/n = 3/1$ external kink modes for each case.

FIG. 10. The global external kink eigenvalues of a dominant $m/n = 3/1$ external kink mode as a function of the ratio of the conducting wall to the plasma diameter

on the cross section at the beginning of a field period for the configurations generated with $I_{hc} = 20kA$ ($\circ$) and $I_{hc} = 180kA$ ($\triangleleft$) at $\beta = 14.4\%$. The magnitude of the eigenvalues reflect the specific kinetic energy normalisation employed in the TERPSICHORE code [16].

FIG. 11. The $2p'(s)\sqrt{g}\boldsymbol{\kappa} \cdot \boldsymbol{\nabla} s$ distribution on a toroidal magnetic surface with $s \sim 0.75$ for the configurations generated with $I_{hc} = 20kA$ (left) and $I_{hc} = 180kA$ (right) at $\beta = 14.4\%$.

FIG. 12. The $\sqrt{g}S$ distribution on a toroidal magnetic surface with $s \sim 0.75$ for the configurations generated with $I_{hc} = 20kA$ (left) and $I_{hc} = 180kA$ (right) at $\beta = 14.4\%$.

FIG. 13. The perturbed pressure distribution on a toroidal magnetic surface near the edge of the plasma dominated by a $m/n = 3/1$ global external kink instability for the configurations generated with $I_{hc} = 20kA$ (left) and $I_{hc} = 180kA$ (right) at $\beta = 14.4\%$. The conducting wall to plasma diameter ratio is $\Delta_W = 2$.

Figure 1:

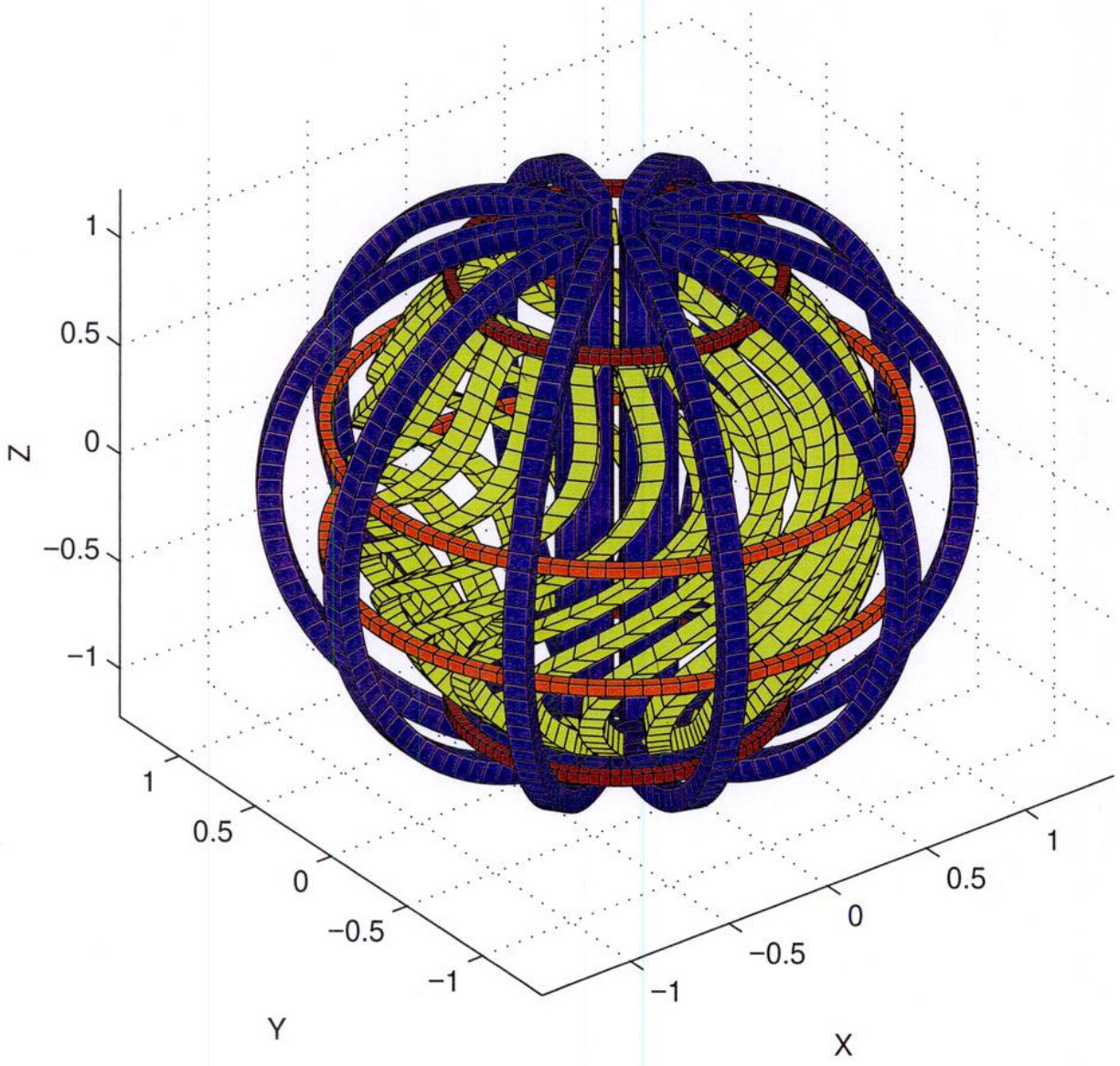

Figure 2:

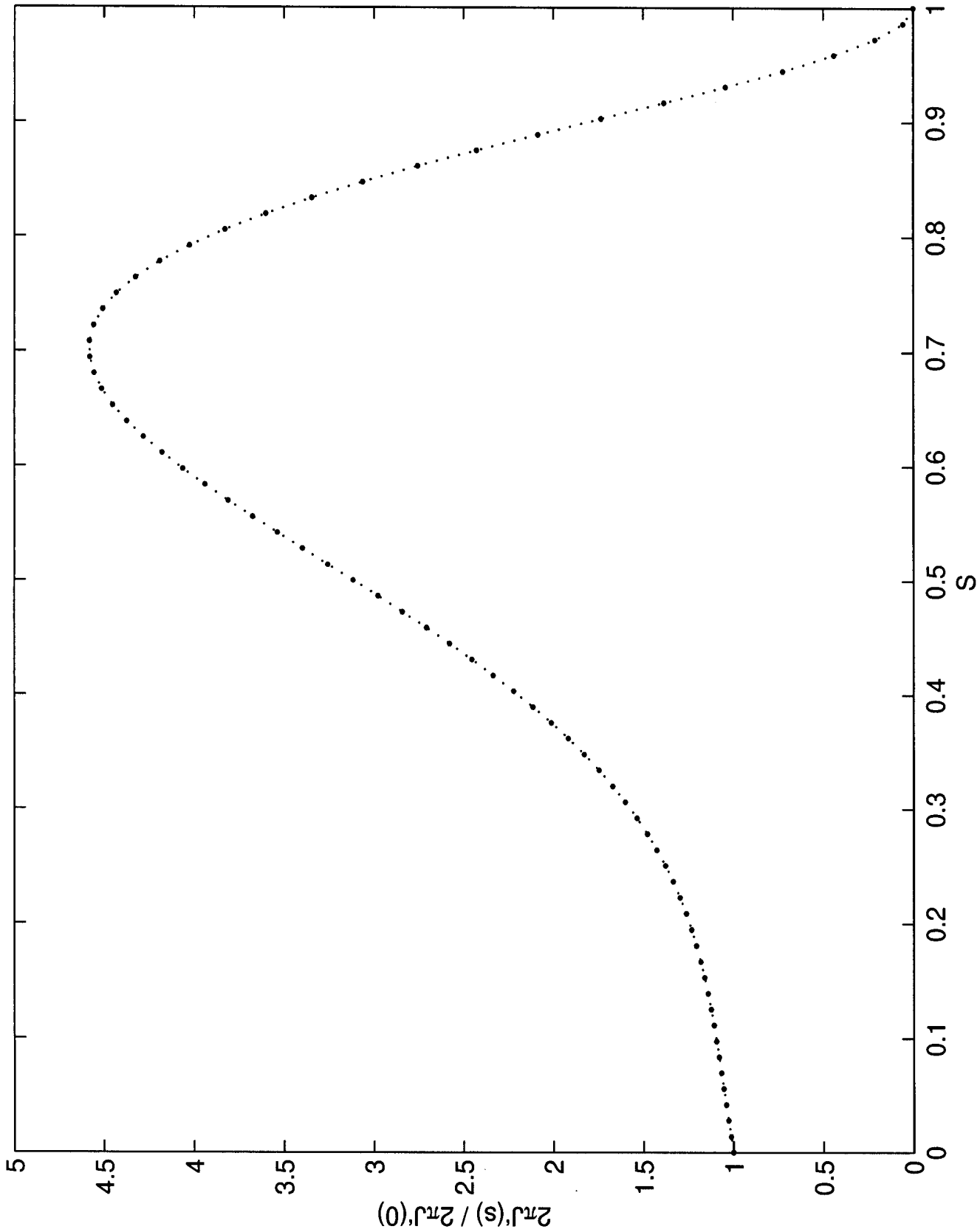

Figure 3:

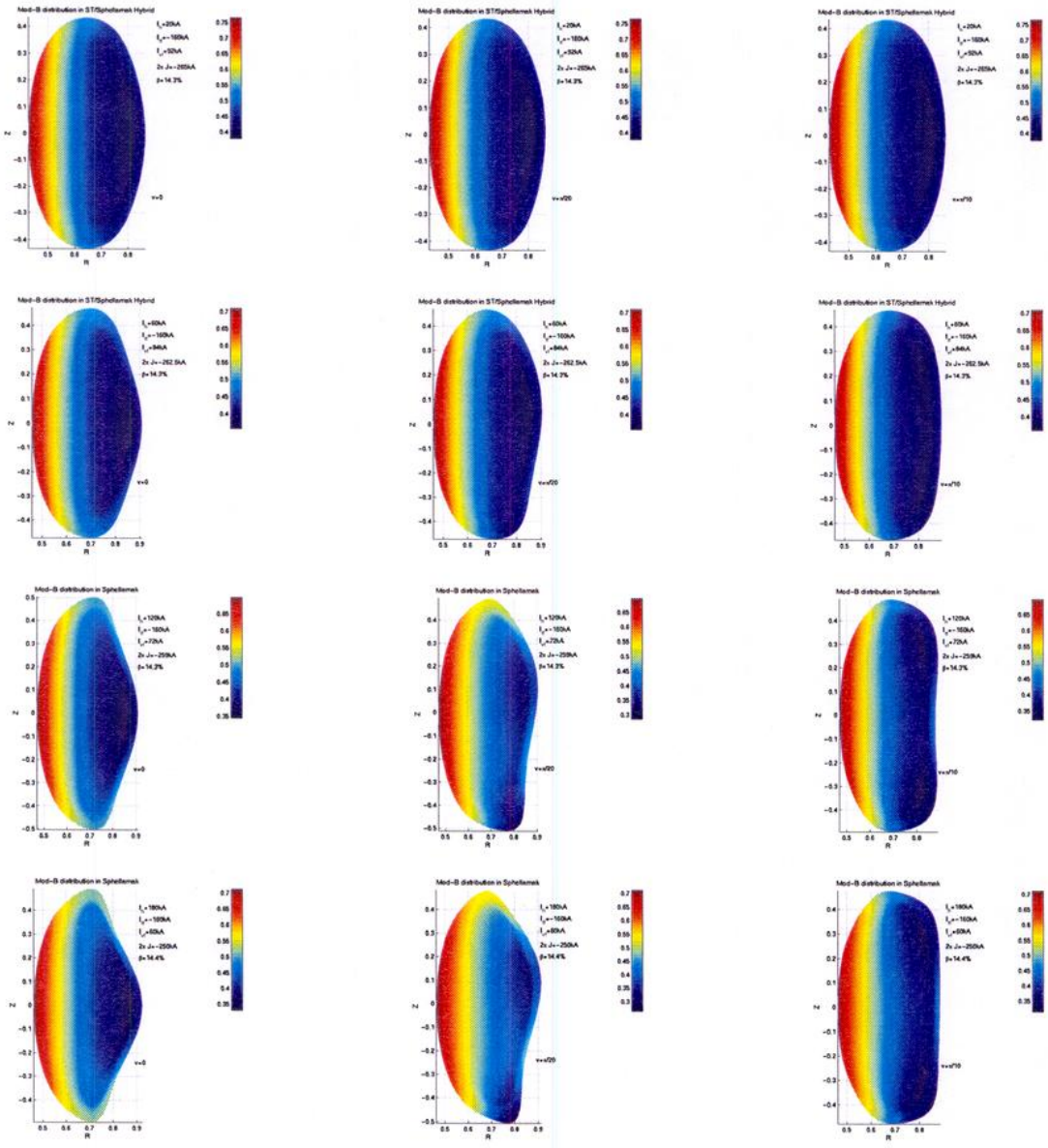

Figure 4:

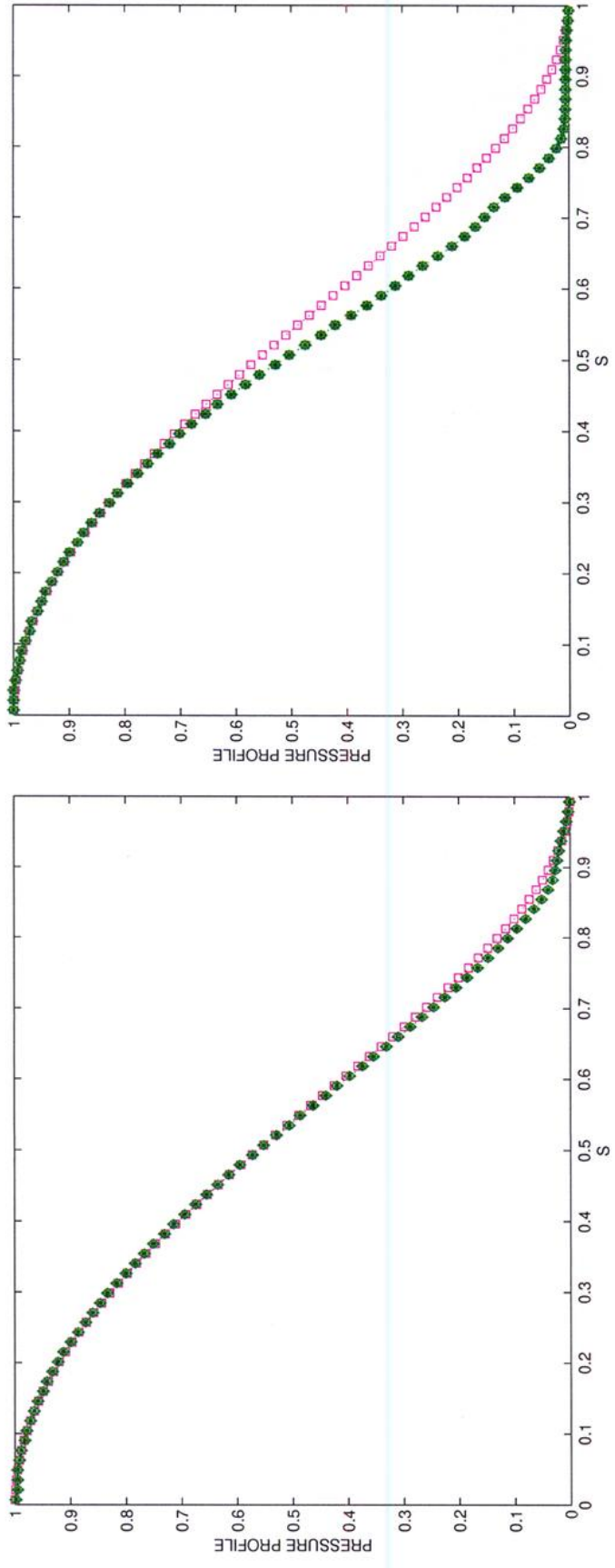
PRESSURE PROFILE
S
0
0.1
0.2
0.3
0.4
0.5
0.6
0.7
0.8
0.9
1
PRESSURE PROFILE
S
0
0.1
0.2
0.3
0.4
0.5
0.6
0.7
0.8
0.9
1

Figure 5:

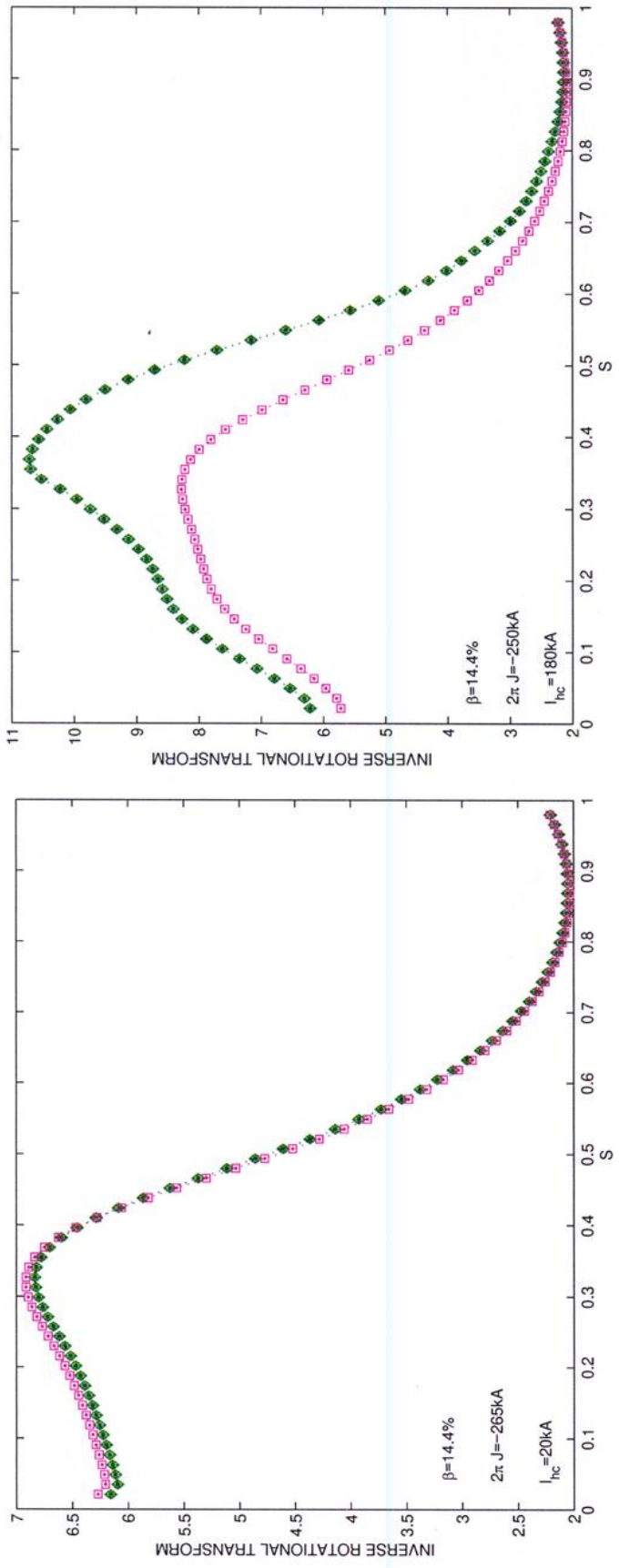
INVERSE ROTATIONAL TRANSFORM
S
β=14.4%
2π J=-250kA
I_hc=180kA
INVERSE ROTATIONAL TRANSFORM
S
β=14.4%
2π J=-265kA
I_hc=20kA

Figure 6:

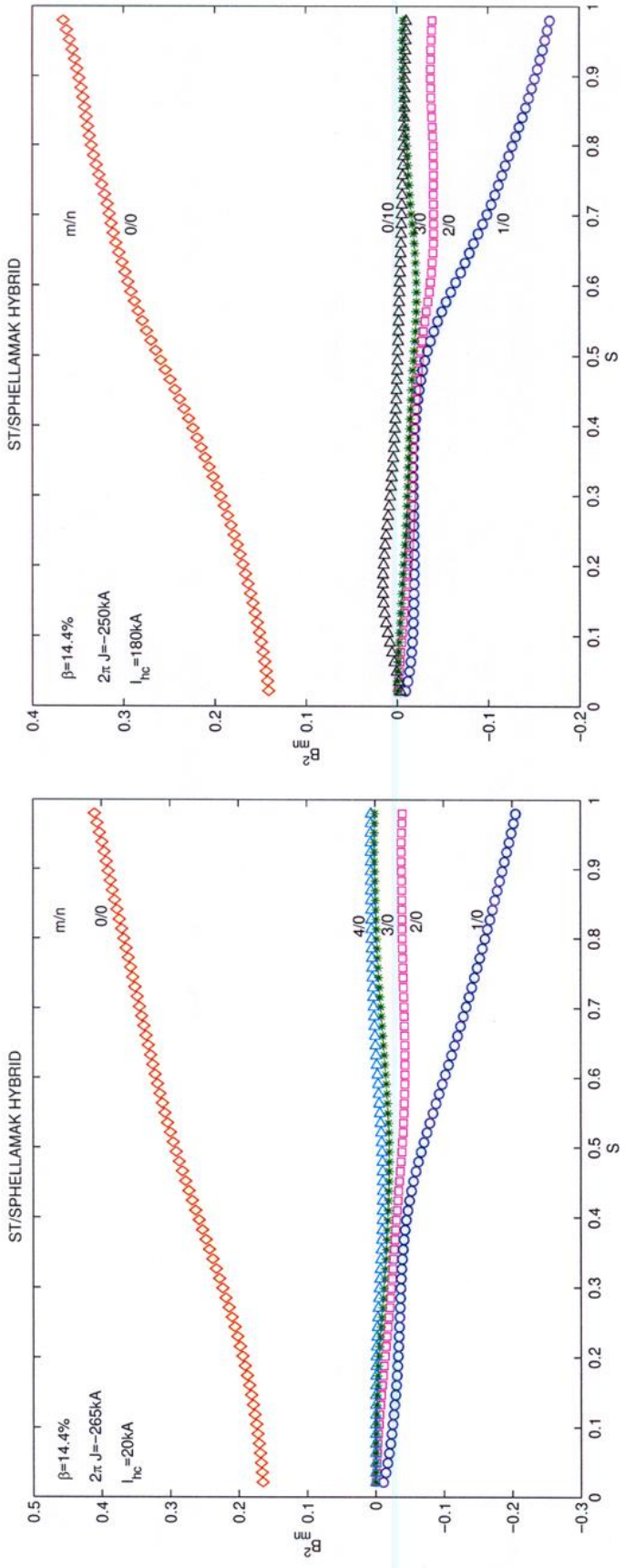
ST/SPHELLAMAK HYBRID
β=14.4%
2π J=−250kA
I_hc=180kA
m/n
0/0
0/10
3/0
2/0
1/0
S
ST/SPHELLAMAK HYBRID
β=14.4%
2π J=−265kA
I_hc=20kA
m/n
0/0
4/0
3/0
2/0
1/0
S

Figure 7:

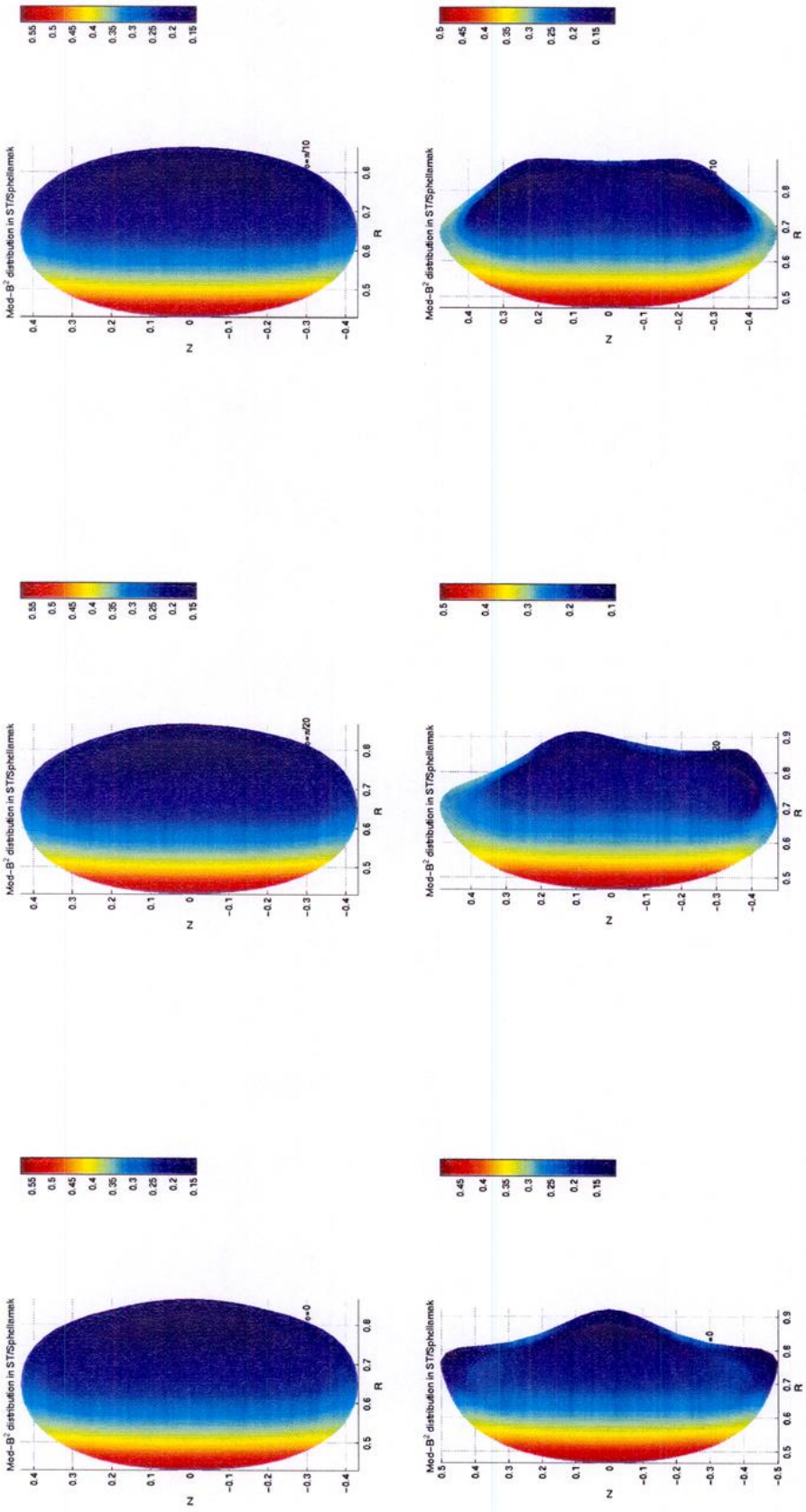

Figure 8:

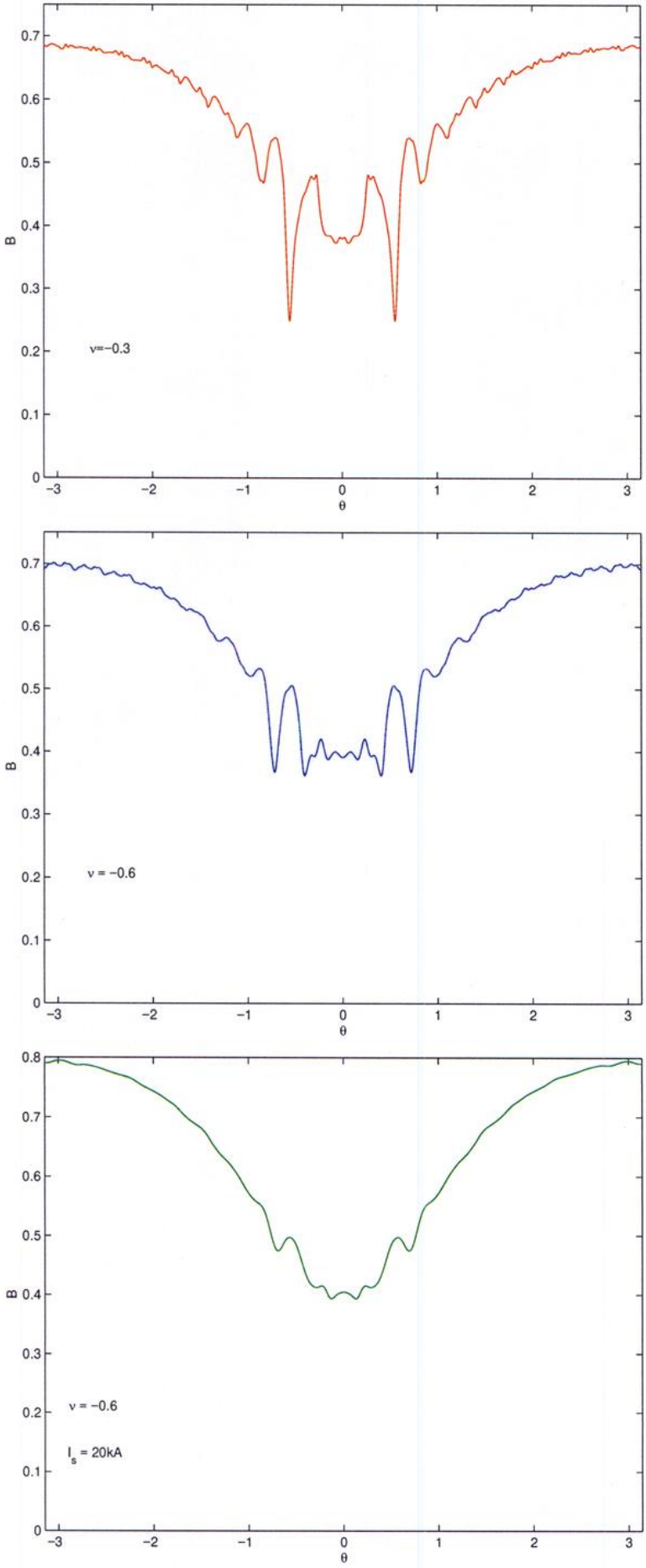

Figure 9:

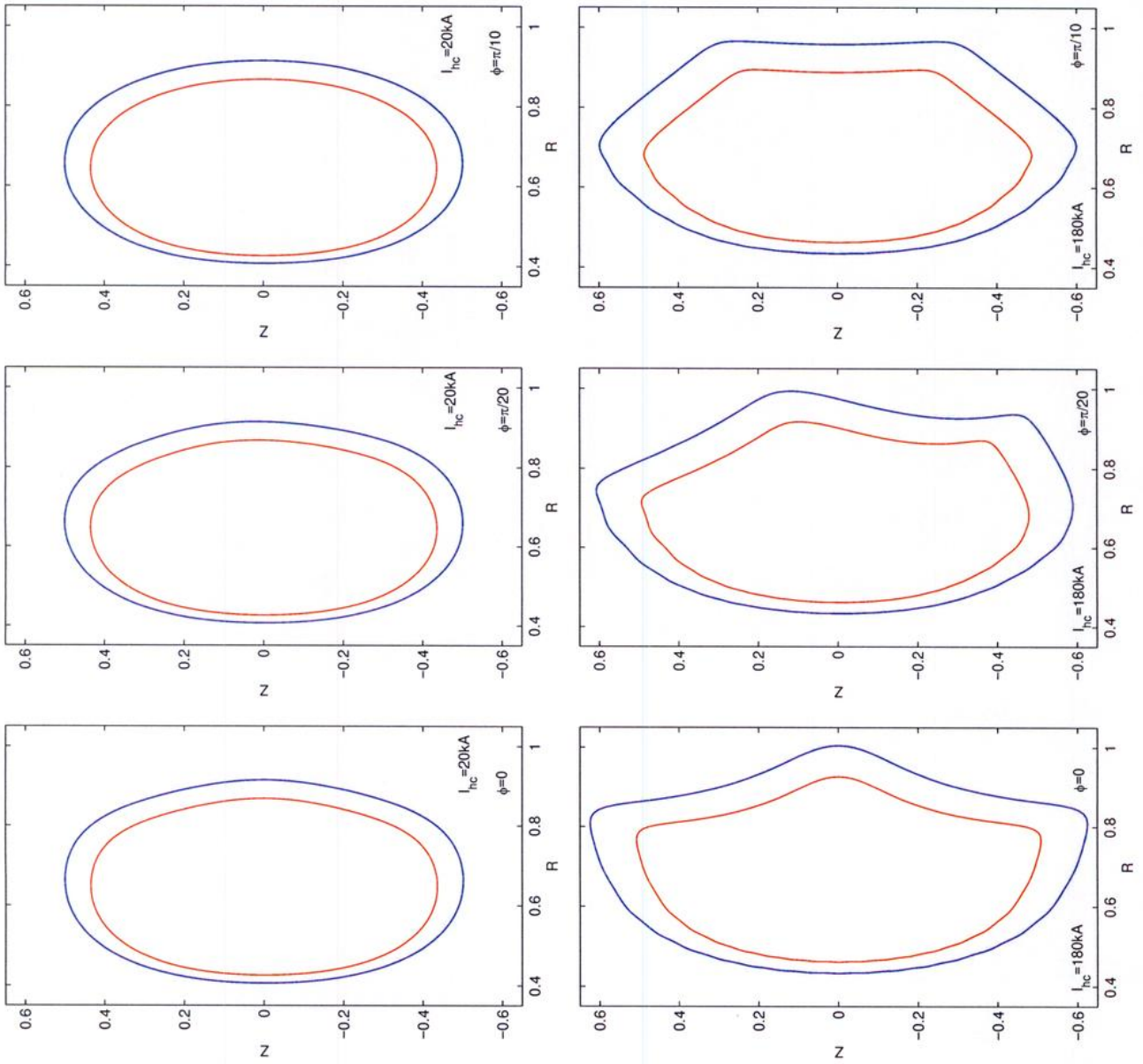
I_hc=20kA
φ=π/10
I_hc=180kA
φ=π/10
I_hc=20kA
φ=π/20
I_hc=180kA
φ=π/20
I_hc=20kA
φ=0
I_hc=180kA
φ=0
R
Z

Figure 10:

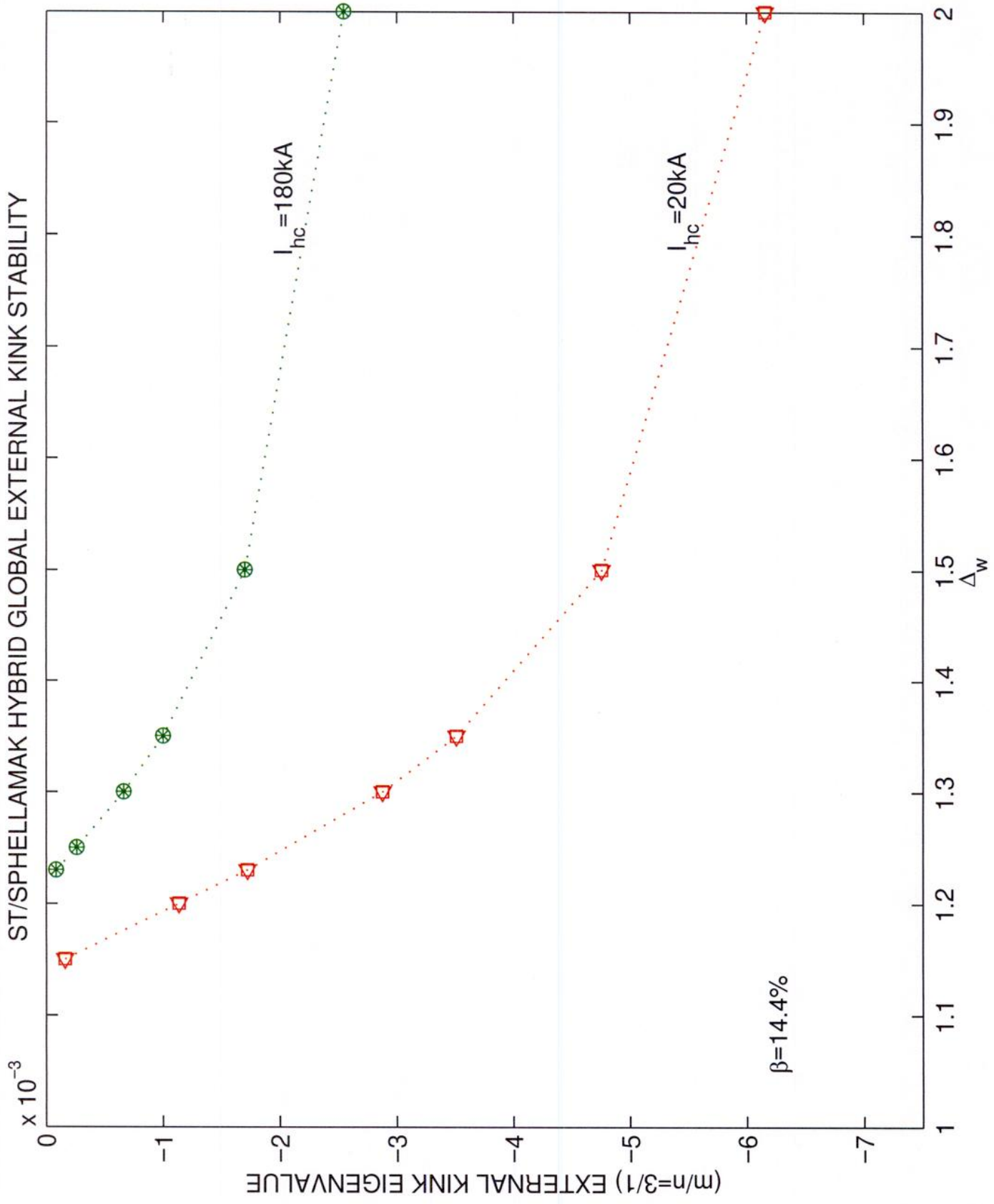
ST/SPHELLAMAK HYBRID GLOBAL EXTERNAL KINK STABILITY
x 10^-3
0
-1
-2
-3
-4
-5
-6
-7
(m/n=3/1) EXTERNAL KINK EIGENVALUE
1
1.1
1.2
1.3
1.4
1.5
1.6
1.7
1.8
1.9
2
Δw
I_hc=180kA
I_hc=20kA
β=14.4%

Figure 11:

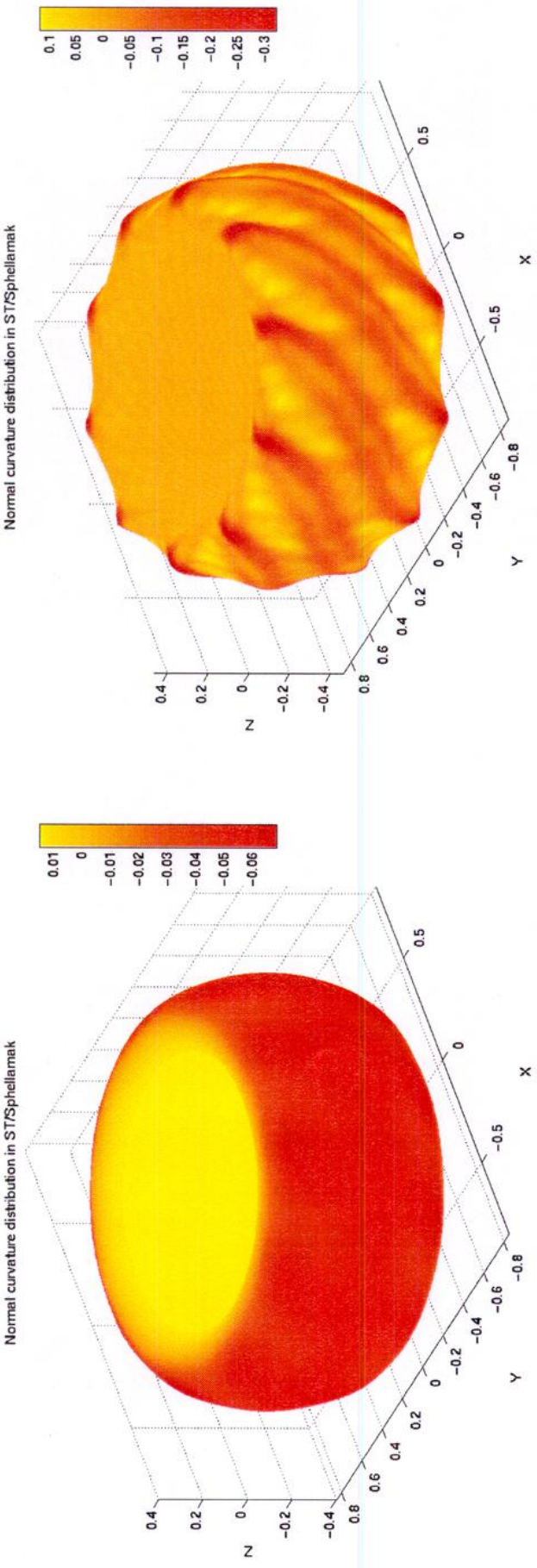
Normal curvature distribution in ST/Sphellamak
0.1
0.05
0
−0.05
−0.1
−0.15
−0.2
−0.25
−0.3
X
Y
Z
Normal curvature distribution in ST/Sphellamak
0.01
0
−0.01
−0.02
−0.03
−0.04
−0.05
−0.06
X
Y
Z

Figure 12:

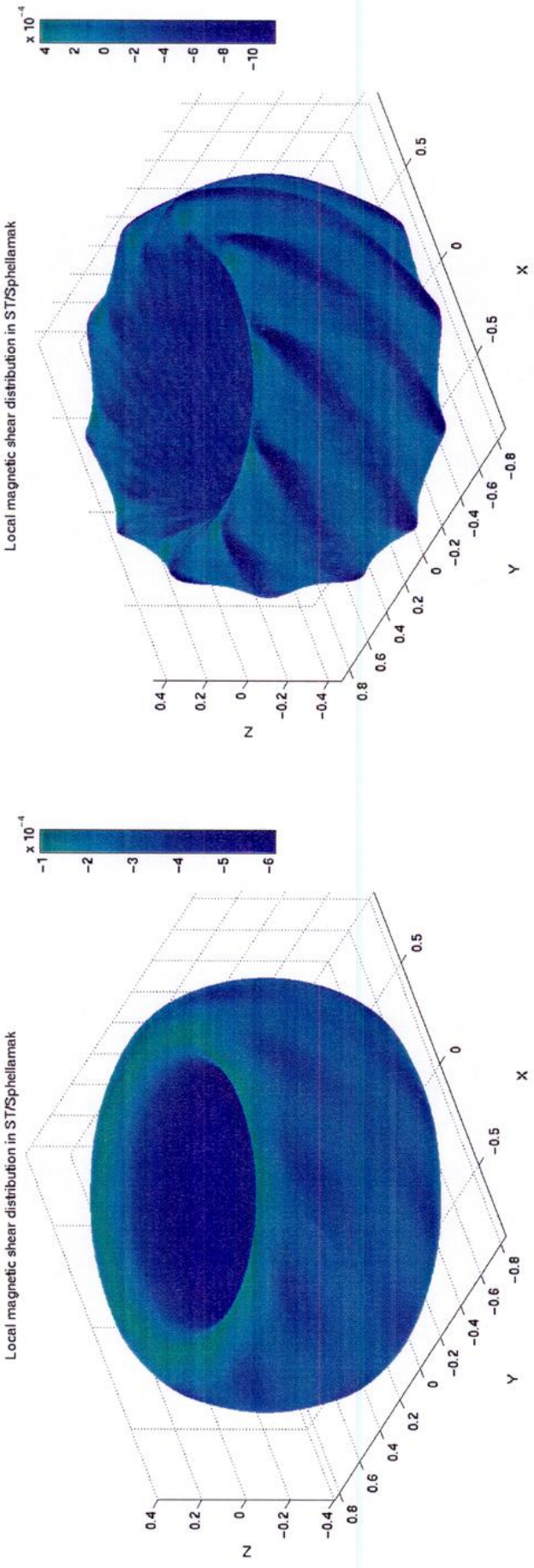
x 10^-4
4
2
0
−2
−4
−6
−8
−10
Local magnetic shear distribution in ST/Sphellamak
X
Y
Z
x 10^-4
−1
−2
−3
−4
−5
−6
Local magnetic shear distribution in ST/Sphellamak
X
Y
Z

Figure 13:

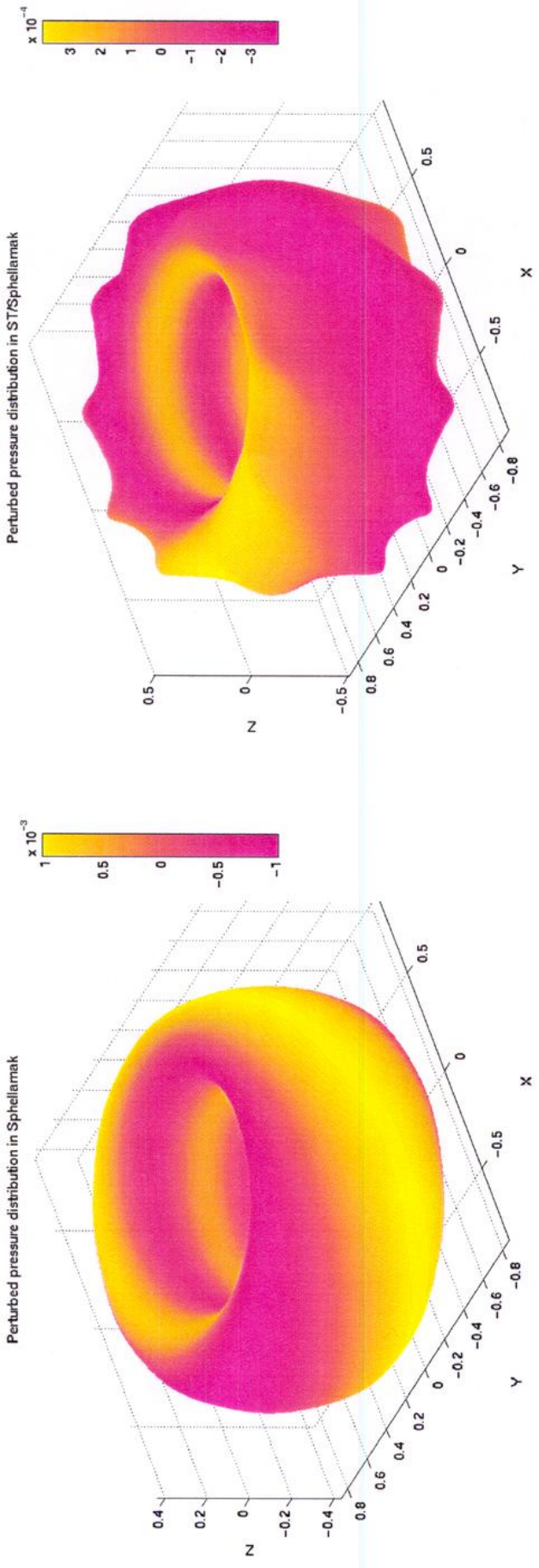
x 10^-4
3
2
1
0
-1
-2
-3
Perturbed pressure distribution in ST/Sphellamak
X
Y
Z
x 10^-3
1
0.5
0
-0.5
-1
Perturbed pressure distribution in Sphellamak
X
Y
Z

Figure 1:

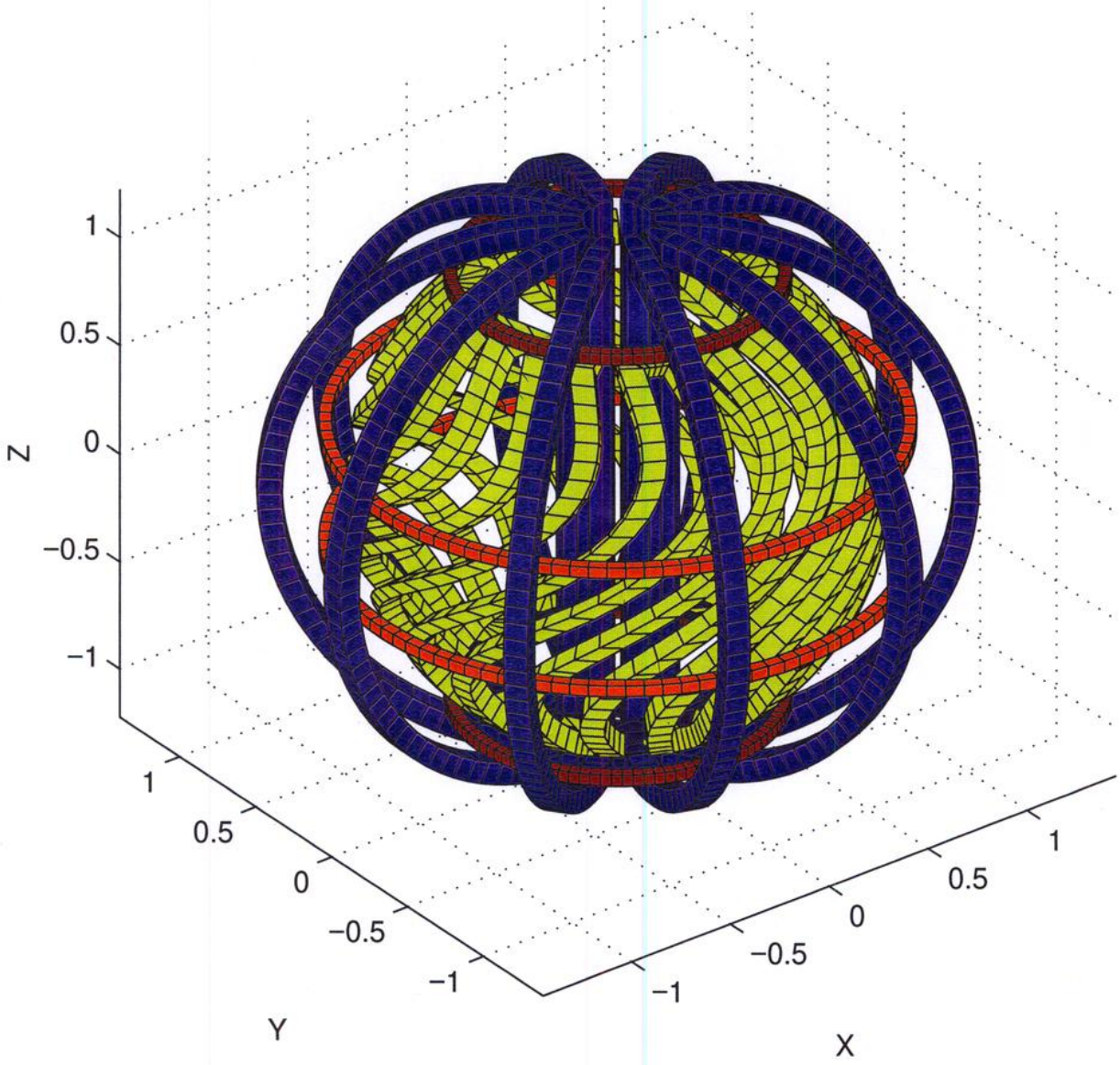

Figure 2:

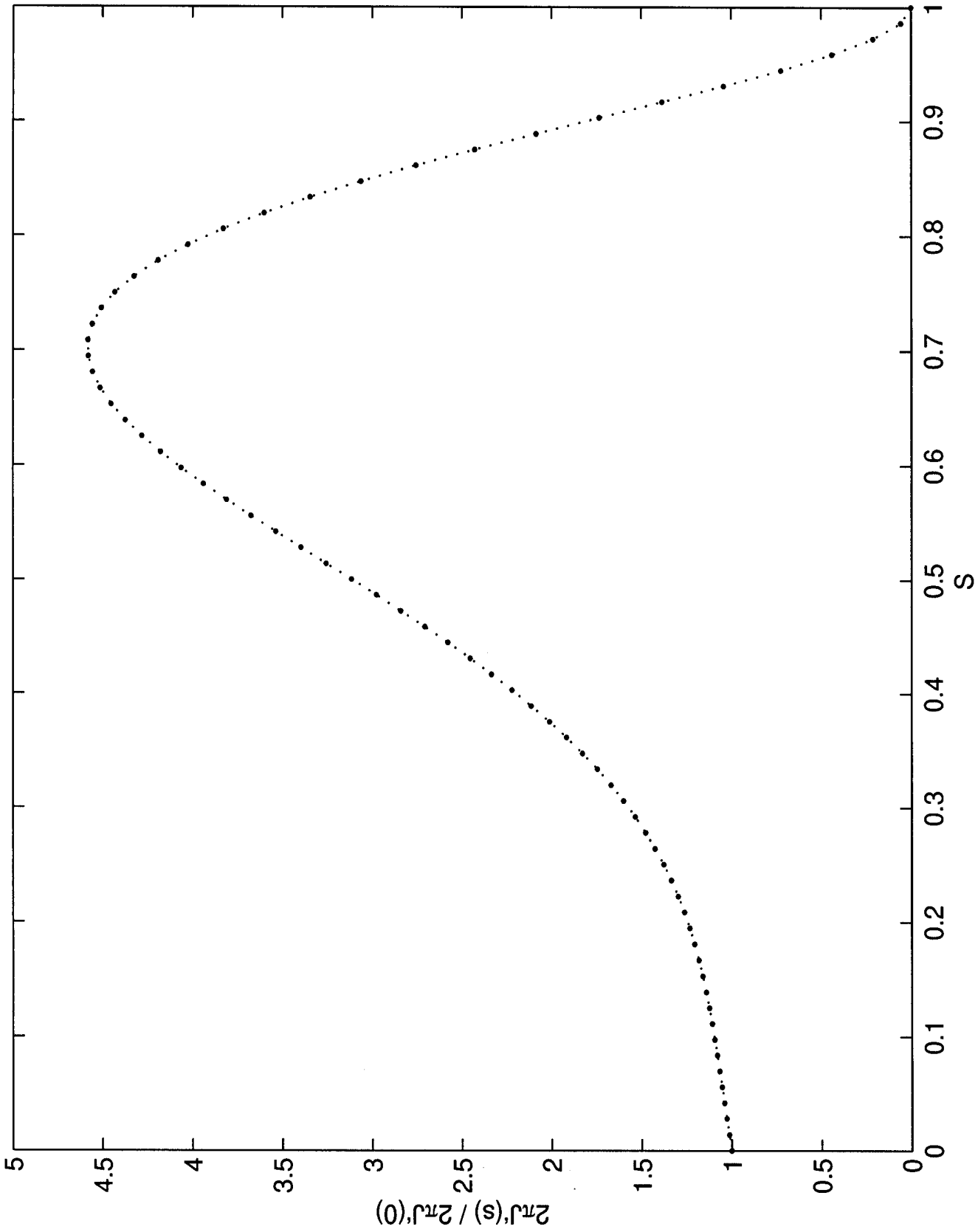

Figure 3:

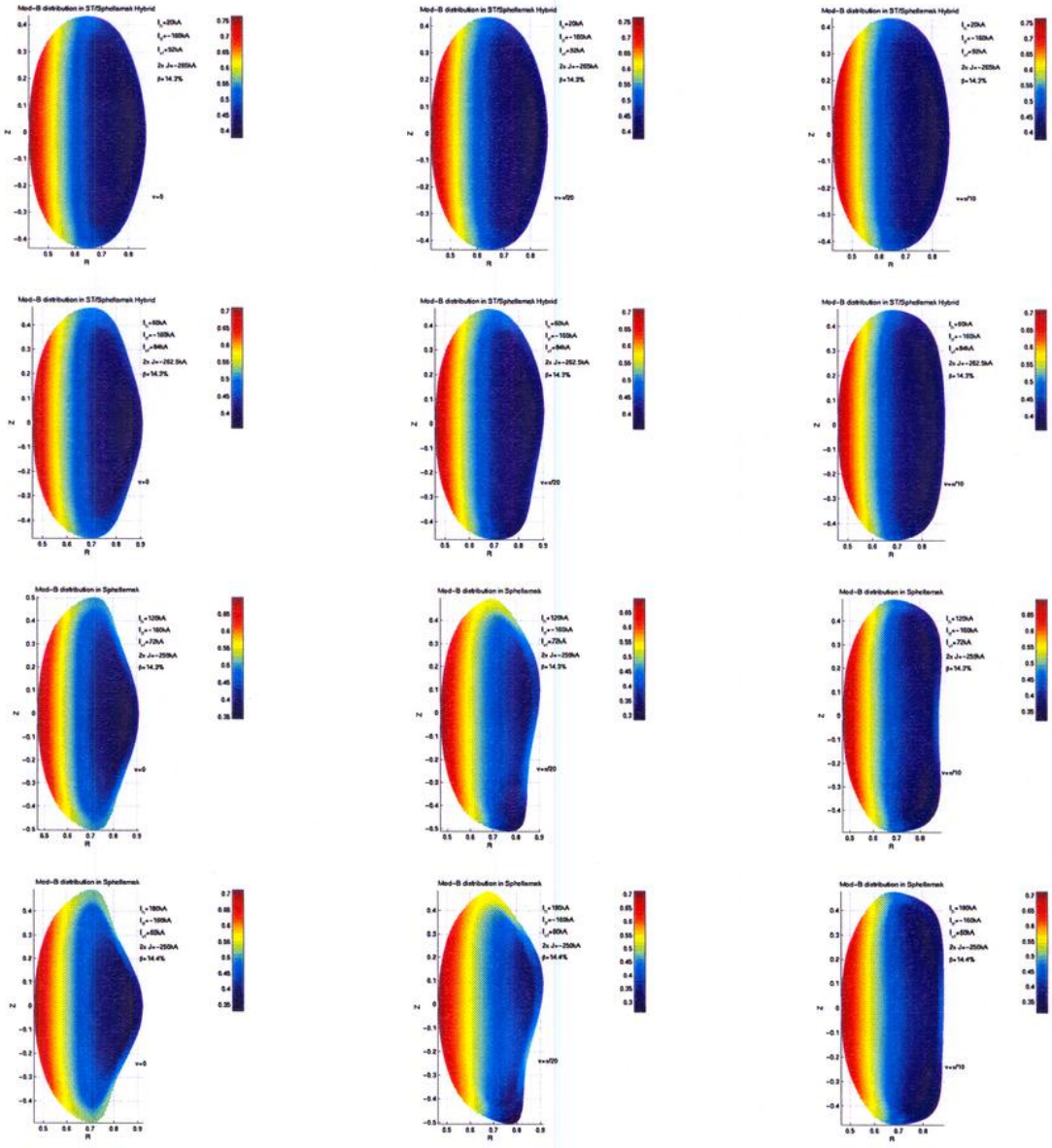

Figure 4:

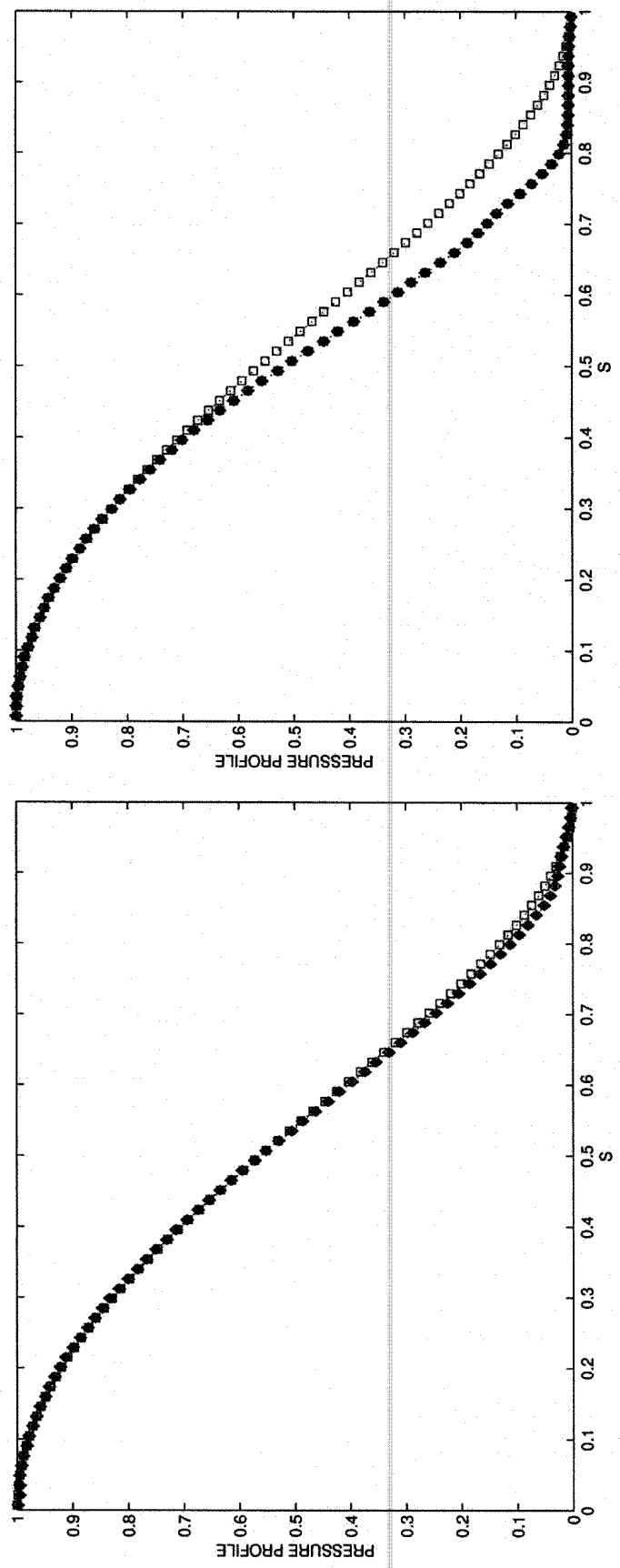
PRESSURE PROFILE
S
0
0.1
0.2
0.3
0.4
0.5
0.6
0.7
0.8
0.9
1
PRESSURE PROFILE
S
0
0.1
0.2
0.3
0.4
0.5
0.6
0.7
0.8
0.9
1

Figure 5:

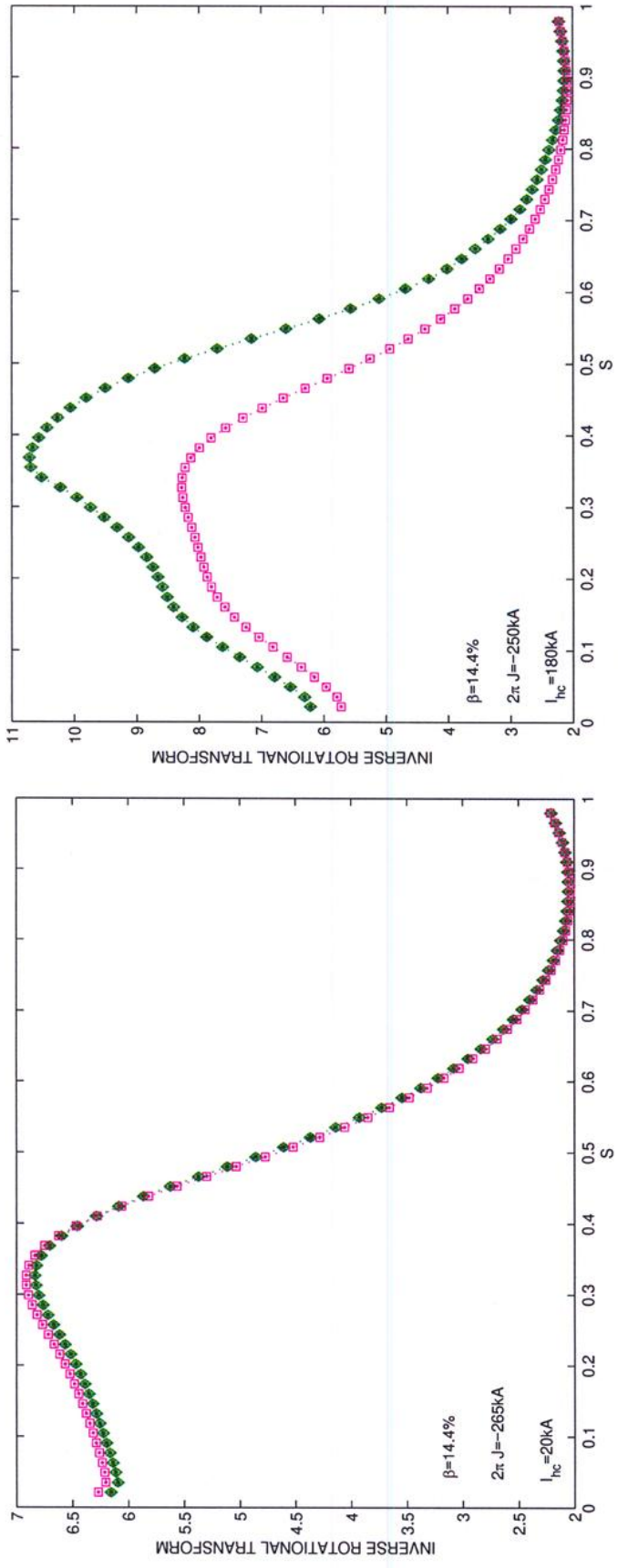
INVERSE ROTATIONAL TRANSFORM
S
β=14.4%
2π J=−250kA
I_hc=180kA
INVERSE ROTATIONAL TRANSFORM
S
β=14.4%
2π J=−265kA
I_hc=20kA

Figure 6:

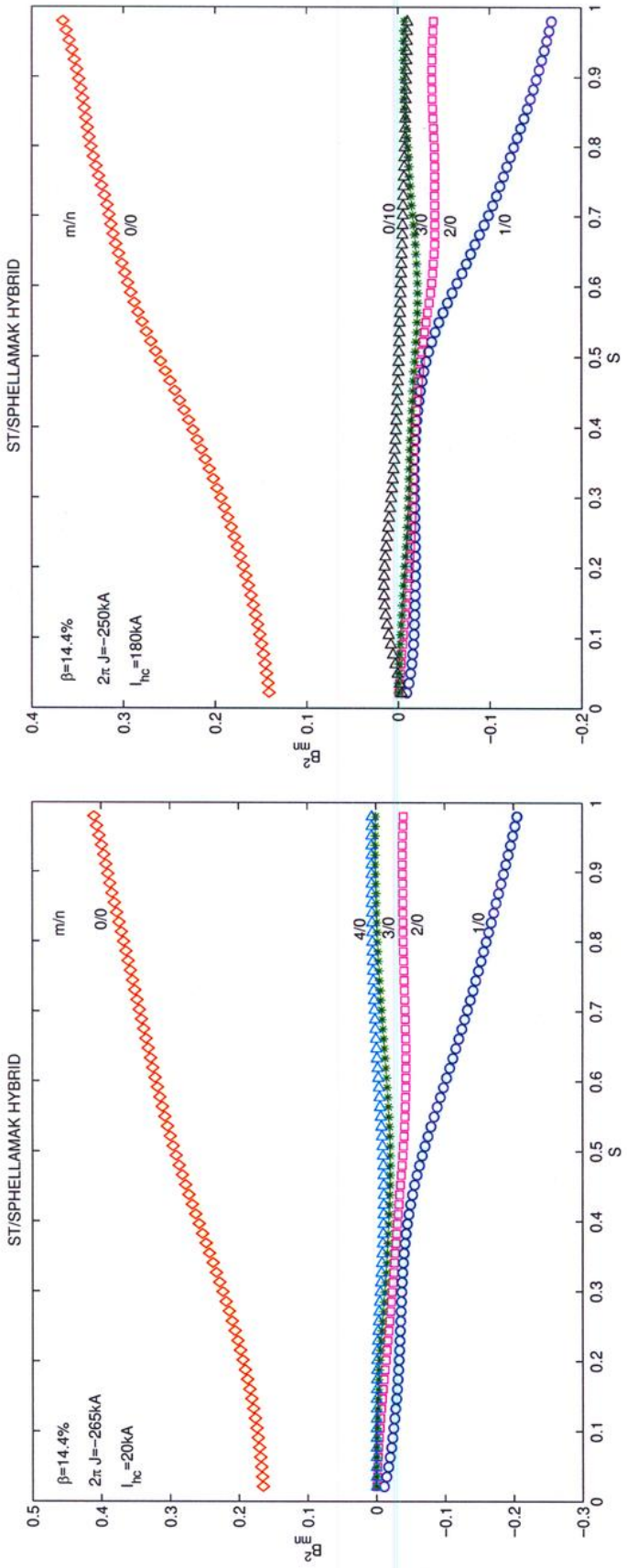
ST/SPHELLAMAK HYBRID
β=14.4%
2π J=−250kA
I_hc=180kA
m/n
0/0
0/10
3/0
2/0
1/0
S
ST/SPHELLAMAK HYBRID
β=14.4%
2π J=−265kA
I_hc=20kA
m/n
0/0
4/0
3/0
2/0
1/0
S

Figure 7:

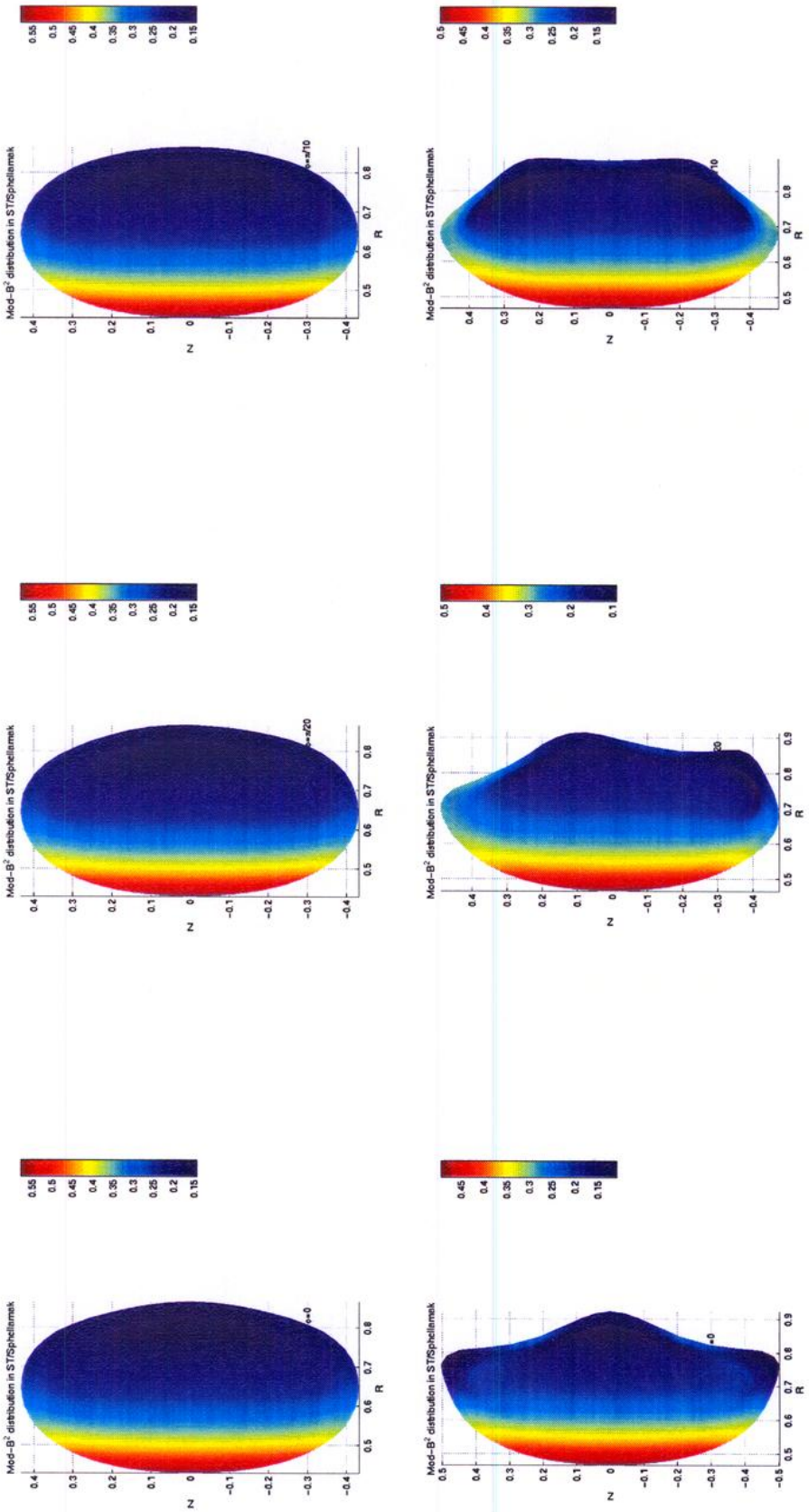

Figure 8:

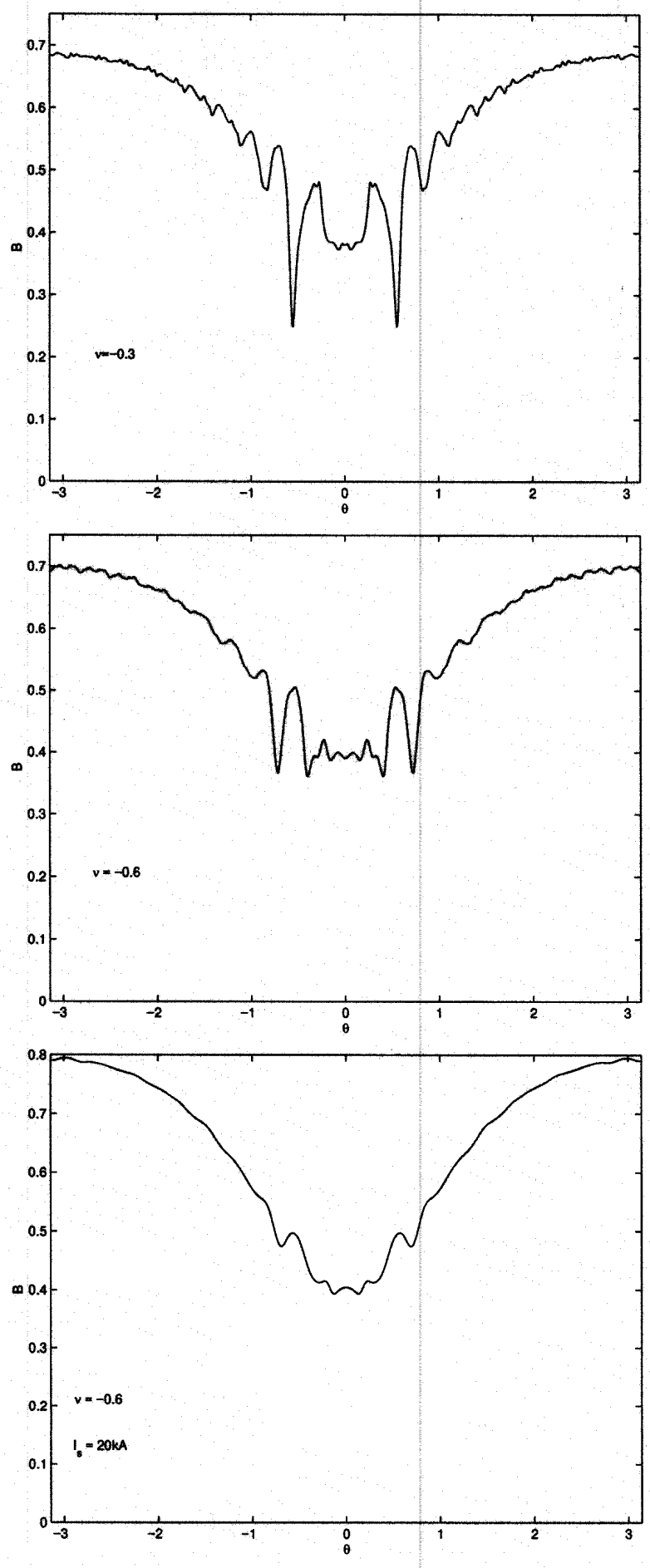

Figure 9:

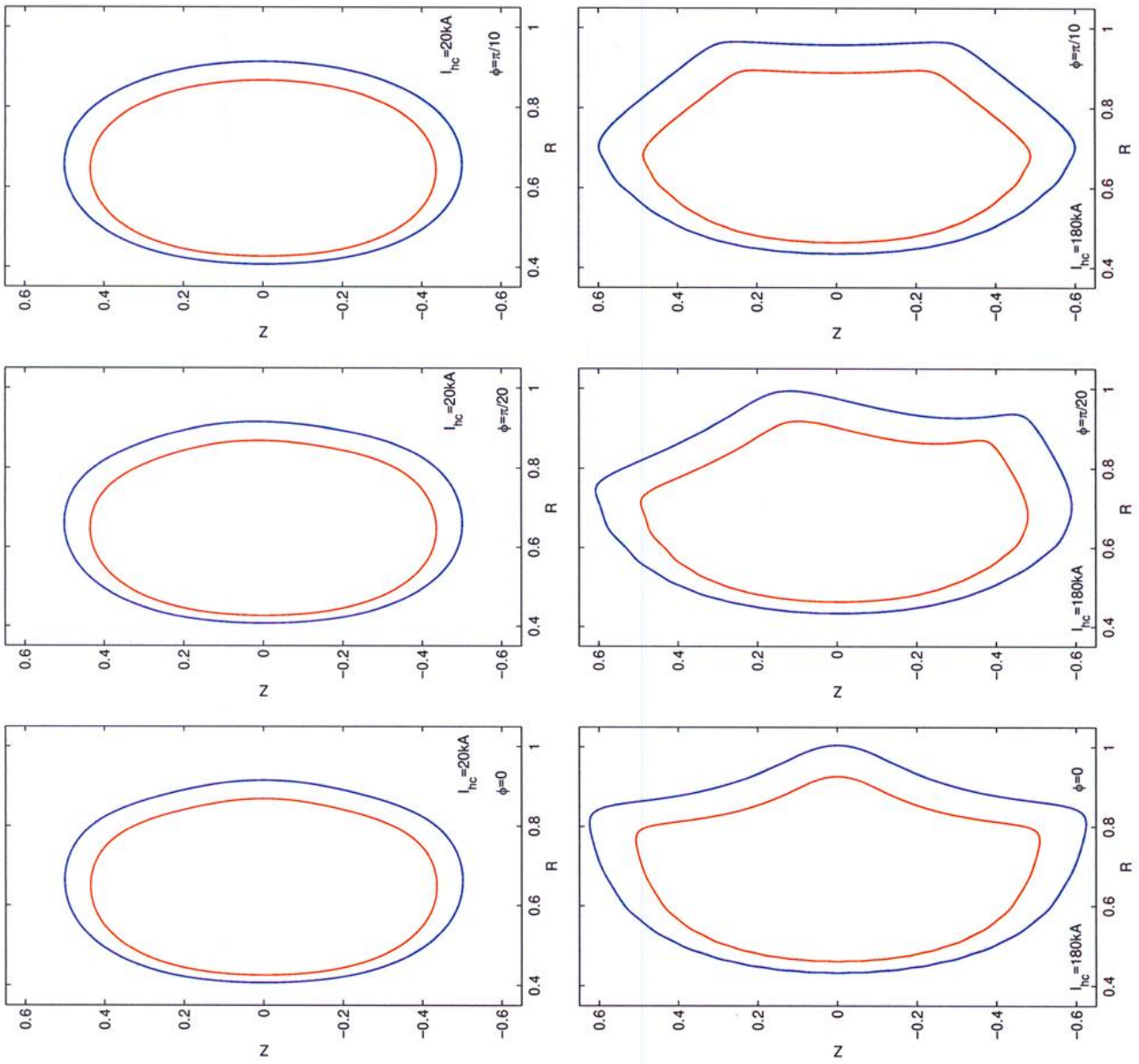
I_hc=20kA
φ=π/10
I_hc=180kA
φ=π/10
I_hc=20kA
φ=π/20
I_hc=180kA
φ=π/20
I_hc=20kA
φ=0
I_hc=180kA
φ=0
R
Z

Figure 10:

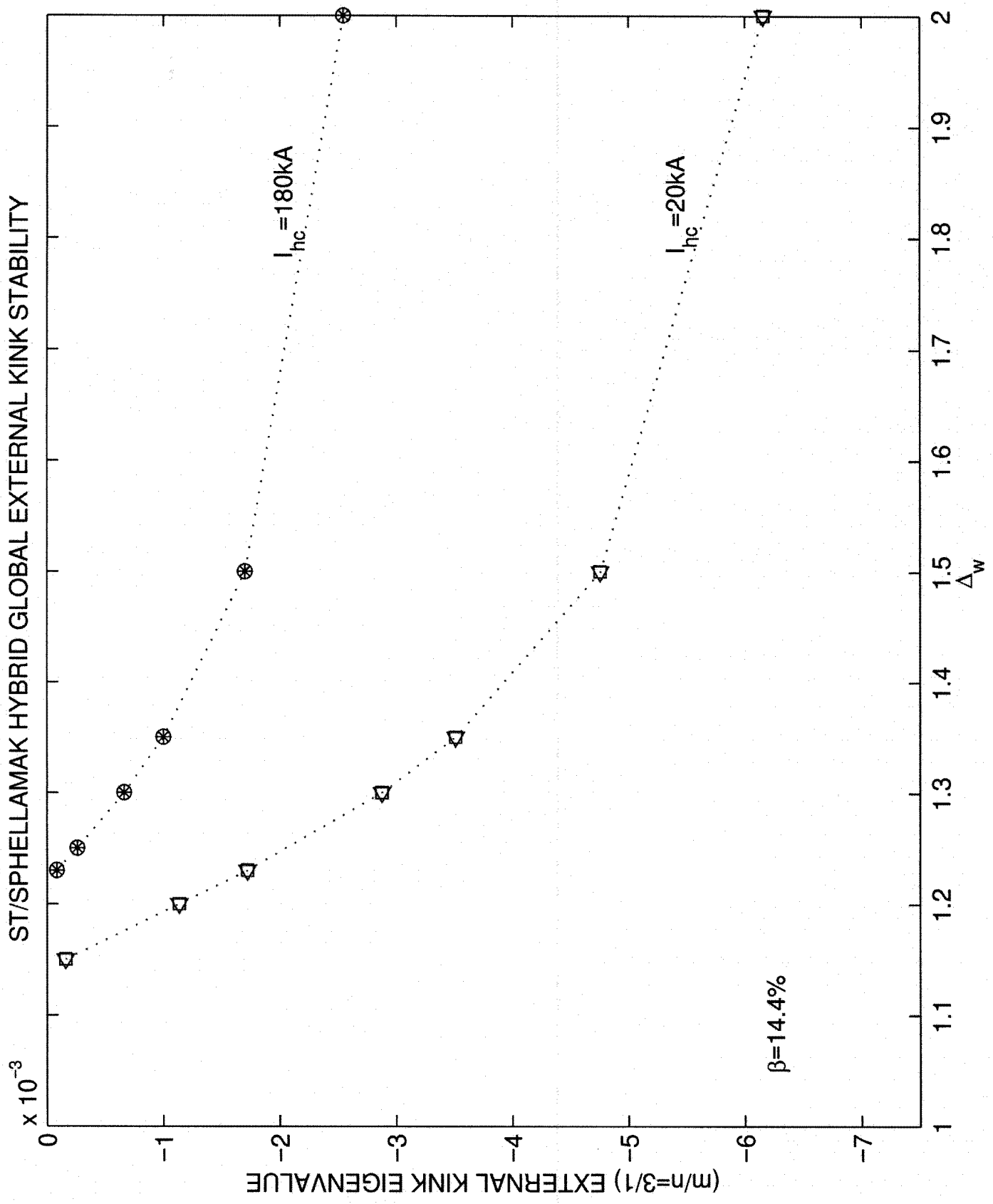
ST/SPHELLAMAK HYBRID GLOBAL EXTERNAL KINK STABILITY
x 10^-3
0
-1
-2
-3
-4
-5
-6
-7
(m/n=3/1) EXTERNAL KINK EIGENVALUE
1
1.1
1.2
1.3
1.4
1.5
1.6
1.7
1.8
1.9
2
Δw
I_hc=180kA
I_hc=20kA
β=14.4%

Figure 11:

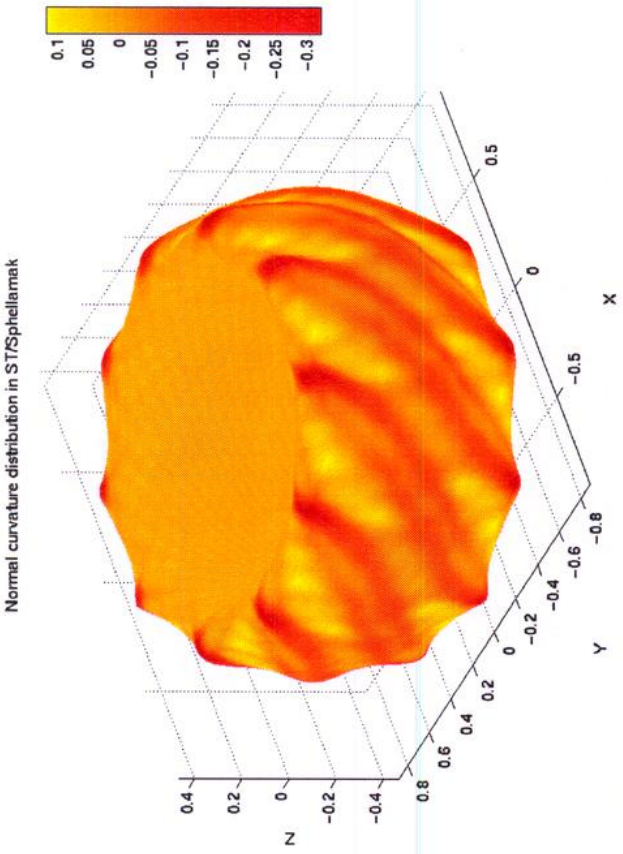
Normal curvature distribution in ST/Sphellamak
0.1
0.05
0
−0.05
−0.1
−0.15
−0.2
−0.25
−0.3
X
Y
Z

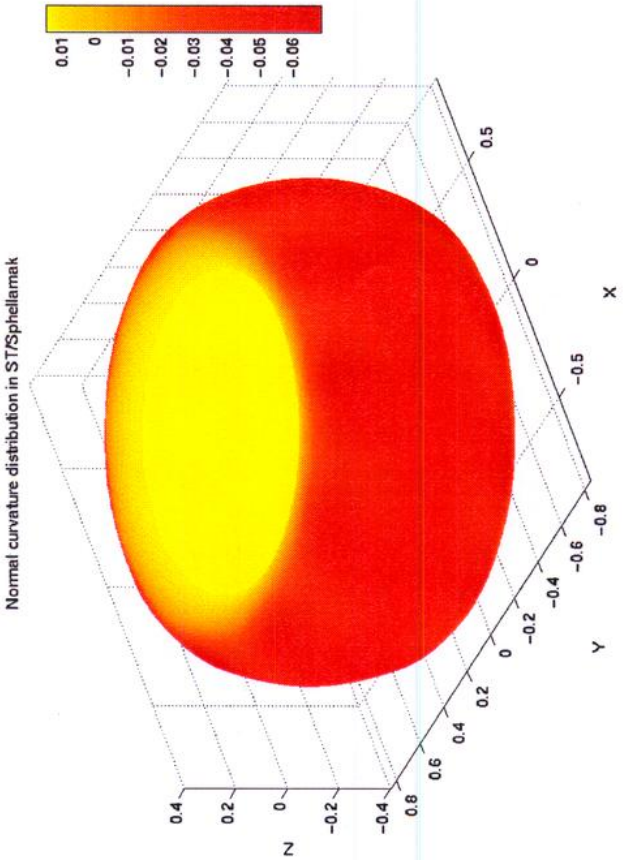
Normal curvature distribution in ST/Sphellamak
0.01
0
−0.01
−0.02
−0.03
−0.04
−0.05
−0.06
X
Y
Z

Figure 12:

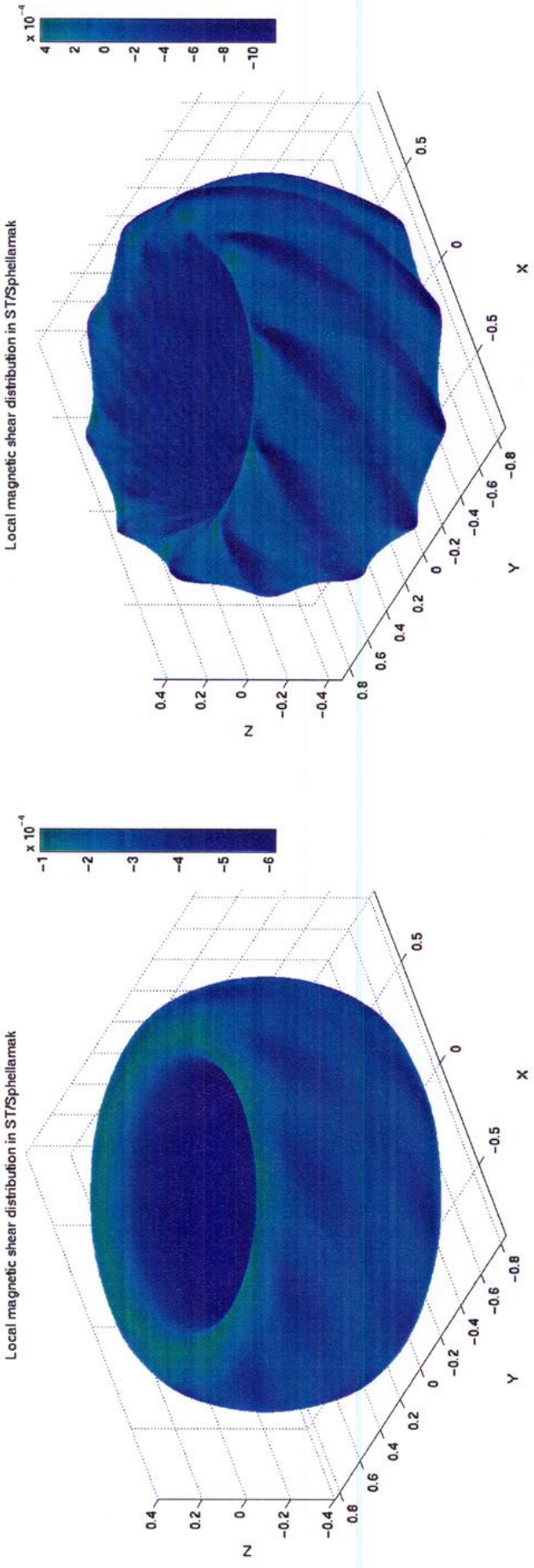
x 10^-4
4
2
0
-2
-4
-6
-8
-10
Local magnetic shear distribution in ST/Sphellamak
X
Y
Z
x 10^-4
-1
-2
-3
-4
-5
-6
Local magnetic shear distribution in ST/Sphellamak
X
Y
Z

Figure 13:

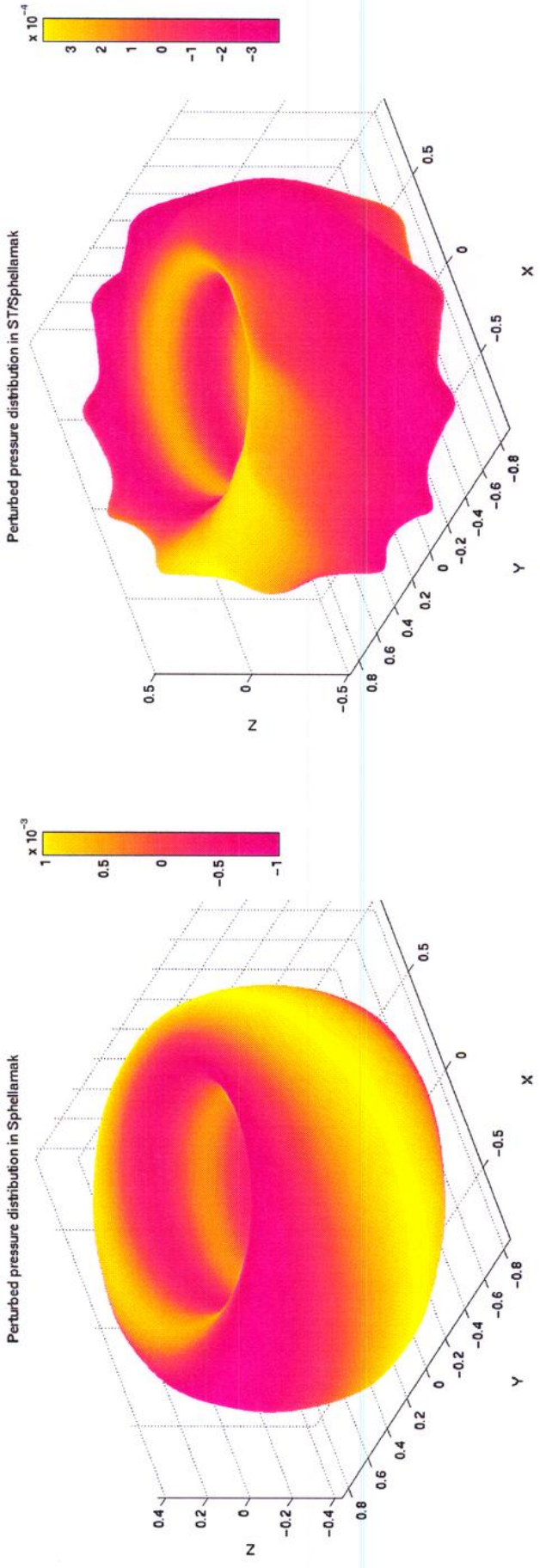
x 10^-4
3
2
1
0
-1
-2
-3
Perturbed pressure distribution in ST/Sphellamak
X
Y
Z
x 10^-3
1
0.5
0
-0.5
-1
Perturbed pressure distribution in Sphellamak
X
Y
Z